THE JOURNAL OF BIOLOGICAL CHEMISTRY VOL. 285, NO. 8, pp. 5776–5791, February 19, 2010

Reciprocal Interactions Regulate Targeting of Calcium Channel β Subunits and Membrane Expression of α_1 Subunits in Cultured Hippocampal Neurons*[S]

Received for publication, July 14, 2009, and in revised form, November 21, 2009 Published, JBC Papers in Press, December 8, 2009, DOI 10.1074/jbc.M109.044271

Gerald J. Obermair[‡1], Bettina Schlick[‡], Valentina Di Biase[‡], Prakash Subramanyam[‡], Mathias Gebhart[§], Sabine Baumgartner[‡], and Bernhard E. Flucher[‡2]

From the [‡]Department of Physiology and Medical Physics, Innsbruck Medical University, and the [§]Department of Pharmacology and Toxicology, University of Innsbruck, 6020 Innsbruck, Austria

Auxiliary β subunits modulate current properties and mediate the functional membrane expression of voltage-gated Ca^{2+} channels in heterologous cells. In brain, all four β isoforms are widely expressed, yet little is known about their specific roles in neuronal functions. Here, we investigated the expression and targeting properties of β subunits and their role in membrane expression of $Ca_V1.2$ α_1 subunits in cultured hippocampal neurons. Quantitative reverse transcription-PCR showed equal expression, and immunofluorescence showed a similar distribution of all endogenous β subunits throughout dendrites and axons. High resolution microscopy of hippocampal neurons transfected with six different V5 epitope-tagged β subunits demonstrated that all β subunits were able to accumulate in synaptic terminals and to colocalize with postsynaptic $Ca_V1.2$, thus indicating a great promiscuity in α_1-β interactions. In contrast, restricted axonal targeting of β_1 and weak colocalization of β_{4b} with $Ca_V1.2$ indicated isoform-specific differences in local channel complex formation. Membrane expression of external hemagglutinin epitope-tagged $Ca_V1.2$ was strongly enhanced by all β subunits in an isoform-specific manner. Conversely, mutating the α-interaction domain of $Ca_V1.2$ (W440A) abolished membrane expression and targeting into dendritic spines. This demonstrates that in neurons the interaction of a β subunit with the α-interaction domain is absolutely essential for membrane expression of α_1 subunits, as well as for the subcellular localization of β subunits, which by themselves possess little or no targeting properties.

Voltage-gated Ca^{2+} channels (Ca_V)[3] provide key pathways for Ca^{2+} entry into neurons and translate membrane depolarization into neurotransmitter secretion and gene regulation. Ca_Vs are composed of a pore-forming α_1 subunit and the auxiliary $\alpha_2\delta$ and β subunits (1). Whereas the α_1 subunits are responsible for voltage sensing and ion conduction, the auxiliary subunits have been implicated in membrane targeting and modulation of channel properties (for review see Ref. 2). Presynaptic Ca_Vs regulate neurotransmitter release (3), and postsynaptic Ca_Vs activate the transcriptional regulators cAMP-response element-binding protein (CREB) and nuclear factor of activated T-cells (NFAT) (4, 5) and thus modulate long term potentiation (6). These functions reflect both the diversity of Ca_V isoforms expressed in brain (7–11) and their differential subcellular localization in neurons (12–15).

Four distinct β isoforms have been identified (16–19), all of which are expressed in brain (20–23). They contain an Src homology 3 domain and a guanylate kinase domain (24–27). However, the guanylate kinase fold is modified so that it can bind with high affinity to the so-called α-interaction domain (AID) in the intracellular I–II linker of Ca_V α_1 subunits (28, 29). The Src homology 3 and the guanylate kinase-like domains are highly conserved among the four genes encoding β subunits (*Cacnb1–b4*; Fig. 1*C*), whereas the sequence connecting these domains as well as the N and C termini are subject to alternative splicing (30, 31). When coexpressed with α_1 subunits in heterologous expression systems, such as *Xenopus laevis* oocytes or human embryonic kidney cells, all four β isoforms modulate the current properties and cause a strong increase in the current density (17–19, 32) by an enhanced functional membrane expression of the channel (33). However, it is not clear whether association of a β subunit is also required for the membrane expression of Ca_Vs in neurons. In skeletal muscle of a β-null zebrafish mutant, for example, this is not the case. There the Ca_Vs are inserted in the membrane and normally target into the triads in the absence of a β subunit (34). Due to the expression of multiple channel isoforms in pre- and postsynaptic compartments, subcellular targeting of Ca_Vs in neurons is highly complex. To date, the only available studies indicate that different β subunits show differential pre- and postsynaptic localization and that this correlates with differential functions in synaptic plasticity (35, 36). Therefore, it is important to determine whether β subunits possess independent targeting properties for neuronal compartments and whether they are involved in the pre- and postsynaptic targeting of Ca^{2+} channels.

Here, we addressed these questions using immunocytochemistry, quantitative RT-PCR, and heterologous expression

* This work was supported by grants from the Austrian Science Fund and the Austrian National Bank Grants P17806-B05, P17807-B05, P20059-B05, P20670, and W1101-B12, and the Tyrolean Science Fund (to G. J. O.).

[S] The on-line version of this article (available at http://www.jbc.org) contains supplemental "Methods," Figs. 1 and 2, and additional references.

[1] To whom correspondence may be addressed. Tel.: 43-512-9003-70841; Fax: 43-512-9003-73800; E-mail: Gerald.Obermair@i-med.ac.at.

[2] To whom correspondence may be addressed. Tel.: 43-512-9003-70836; Fax: 43-512-9003-73836; E-mail: bernhard.e.flucher@i-med.ac.at.

[3] The abbreviations used are: Ca_V, voltage-gated Ca^{2+} channel; AID, α-interaction domain; BSA, bovine serum albumin; eGFP, enhanced green fluorescent protein; HA, hemagglutinin; RT, reverse transcription; PBS, phosphate-buffered saline; ANOVA, analysis of variance; DIV, days *in vitro*; pβA, β-actin promoter.

of epitope-tagged Ca_Vs in cultured hippocampal neurons. We demonstrate that all β isoforms are expressed at similar levels, display similar distribution patterns, and can colocalize with pre- and postsynaptic α_1 subunits. Nevertheless, differences in axonal targeting and isoform-specific effects on membrane expression of $Ca_V1.2$ suggest the existence of preferential α_1-β partners in neurons. Together our data demonstrate for the first time that in neurons the subcellular localization of β subunits primarily depends on their association with an α_1 subunit, suggesting that β subunits are not involved in synaptic targeting of Ca^{2+} channels. On the other hand, as shown previously in heterologous cells, also in neurons the association of β subunits with the AID domain is essential for membrane expression of the postsynaptic $Ca_V1.2$.

EXPERIMENTAL PROCEDURES

Cell Culture and Transfection

Low density cultures of hippocampal neurons were prepared from 16.5-day-old embryonic BALB/c mice as described previously (15, 37, 69). Plasmids were introduced into neurons on day 6 using Lipofectamine 2000 transfection reagent (Invitrogen) as described previously (15). For single transfection experiments (pβA-β-V5 constructs), 0.5–2 μg of DNA at a molar ratio of 1:1 were used, and for cotransfection experiments (pβA-eGFP, pβA-$Ca_V1.2$-HA, and pβA-βx-V5), 1–2.5 μg of total DNA at a molar ratio of 1:1 were used. Cells were immunostained and analyzed 6–19 days after transfection.

Molecular Biology

All constructs were cloned into a eukaryotic expression plasmid containing a neuronal chicken β-actin promoter (pβA; see Refs. 15, 38). For details about sources and cloning strategies of all constructs used in this study, see supplemental Methods. The GenBank™ accession numbers used were as follows: β_{1a}, M25514 (16); β_{1b} X61394 (39); β_{2a}, M80545 (17); β_{2b}, AF423193 (30); β_3, NM_012828 (19); and β_{4b}, L02315 (18).

Quantitative TaqMan RT-PCR

RNA Isolation and Reverse Transcription—2-Week-old BALB/c mice were euthanized by CO_2 exposure, and brains were excised after decapitation. Brain regions were dissected in cold Hanks' buffered saline solution, and total RNA was extracted from homogenized brain tissue using the RNeasy protect mini kit (Qiagen, GmbH, Hilden, Germany). To isolate RNA from hippocampal neurons, cultures (24 DIV) were harvested by trypsin treatment; total RNA was extracted as described above, and RNA concentrations were determined photometrically. Reverse transcription was performed with 1 μg (hippocampi) or 5 μl (cultured neurons) of RNA using Superscript II reverse transcriptase (Invitrogen) and random primers (Promega, Madison, WI); the RT mixture was incubated for 60 min at 37 °C.

Quantitative TaqMan RT-PCR—The relative abundance of different β transcripts was assessed by quantitative RT-PCR using a standard curve method as described elsewhere (40, 41).[4] The following specific TaqMan gene expression assays, designed to span exon-exon boundaries, were purchased from Applied Biosystems (Foster City, CA): β_1, Mm00518940_m1; β_2, Mm00659092_m1; β_3, Mm00432233_m1; and β_4, Mm00521623_m1. The following primers (MWG Biotec, Ebersberg, Germany) were used for PCR amplification of assay-specific fragments using whole brain cDNA as a template (where F is forward and R is reverse): β_1 F, 5′-gatcctctccatggtccagaa-3′, and β_1 R, 5′-ctgcctccttccttaaggcttc-3′; β_2 F, 5′-gactatctggaggcatactggaag-3′, and β_2 R, 5′-ctctcttgggtttcagagtcaaa-3′; β_3 F, 5′-cccatgtatgacgactcctacg-3′, and β_3 R, 5′-acagtagctgacattggtcctcac-3′; β_4 F, 5′-gctgattaagtccagaggaaagtc-3′, and β_4 R, 5′-tgtctcattcgctgactctgtaat-3′. The integrity of the obtained fragments was confirmed by sequencing (MWG Biotec). To calculate standard curves, fragment concentrations were determined in a TECAN Genios Microplate Reader (Tecan Group Ltd., Männedorf, Switzerland) using the Quant-IT PicoGreen double-stranded DNA reagent (Invitrogen) according to the manufacturer's instructions. Standard curves with 10-fold serial dilutions from 10^7 to 10 molecules of the respective fragment were generated for each assay. Quantitative RT-PCR was performed in triplicate measurements using 20 ng of total RNA equivalents of cDNA and the specific TaqMan gene expression assay in a final volume of 20 μl in TaqMan universal PCR master mix (Applied Biosystems). To compare the relative expression of Ca_V β subunits between hippocampus and the cultured neurons, data were normalized to *Hprt1* expression (Mm00446968_m1). *Hprt1* was determined to be the most stable control gene among 7 genes tested (data not shown). Analysis was performed using the ABI PRISM 7500 sequence detector (Applied Biosystems).

Immunocytochemistry

Neurons were fixed in pF (pF: 4% paraformaldehyde, 4% sucrose) in PBS at room temperature. Fixed neurons were incubated in 5% normal goat serum in PBS/BSA/Triton (PBS containing 0.2% BSA and 0.2% Triton X-100) for 30 min. Primary antibodies were applied in PBS/BSA/Triton at 4 °C overnight and detected by fluorochrome-conjugated secondary antibodies (15). For staining of surface-expressed HA-tagged $Ca_V1.2$ constructs, living neurons were incubated with the rat anti-HA antibody for 30 min at 37 °C (42, 43). Then the cultures were rinsed in Hanks' buffered saline solution, fixed for 10 min with pF, blocked with normal goat serum, and incubated with the secondary antibody for 1 h (15).

For colocalization analysis of surface-expressed $Ca_V1.2$-HA constructs and cytoplasmic β subunits, live cell-stained neurons were postfixed for 5 min in pF. Then neurons were rinsed in PBS, permeabilized, blocked again with 5% normal goat serum in PBS/BSA/Triton, and subsequently incubated with the second primary antibody overnight at 4 °C. After washing, the Alexa 488-conjugated secondary antibody was applied for 1 h at room temperature. Coverslips were then washed and mounted in *p*-phenylenediamine glycerol to retard photobleaching (44). Preparations were analyzed on an Axiophot or an AxioImager microscope (Carl Zeiss, Inc) using ×63, 1.4 NA,

[4] B. Schlick, B. E. Flucher, and G. J. Obermair, submitted for publication.

TABLE 1

Intensity analyses of β_x-V5 subunit distribution in the dendrite (dendrite/soma ratio), the distal axon (axon/soma ratio), and the axon hillock (axon hillock/dendrite ratio)

Numbers of neurons analyzed are given in parentheses. For each condition 2–10 neurons were analyzed in 3–6 independent culture preparations and transfections; means are on first line ± S.E. (italics below).

	β_{1a}	β_{1b}	β_{2a}	β_{2a}-SS	β_{2b}	β_3	β_{4b}
Dendrite[a]	0.20	0.21	0.43[b]	0.17	0.22	0.28	0.24
	0.02	*0.03*	*0.03*	*0.01*	*0.02*	*0.02*	*0.03*
	(24)	(24)	(20)	(21)	(21)	(26)	(23)
Axon[c]	0.015[d]	0.005[e]	0.030	0.036	0.049	0.038	0.051
	0.003	*0.001*	*0.003*	*0.008*	*0.012*	*0.006*	*0.007*
	(19)	(24)	(14)	(15)	(20)	(25)	(20)
Axon hillock[f]	0.73	1.01	1.06	2.84[g]	2.27[g]	0.90	2.64[g]
	0.06	*0.09*	*0.08*	*0.24*	*0.22*	*0.06*	*0.22*
	(24)	(24)	(20)	(21)	(21)	(26)	(23)

[a] ANOVA is as follows: $F_{(6,152)} = 13.3$; $p < 0.001$.
[b] Post hoc (Tukey) is as follows: other βs, $p < 0.001$.
[c] ANOVA is as follows: $F_{(6,130)} = 7.0$; $p < 0.001$.
[d] Post hoc (Tukey) is as follows: β_{2b}, $p = 0.008$; β_{4b}, $p = 0.005$.
[e] Post hoc (Tukey) is as follows: β_{2a}-SS, $p = 0.029$; β_{2b}, β_{4b}, $p < 0.001$; β_3, $p = 0.003$.
[f] ANOVA is as follows: $F_{(6,152)} = 34.1$; $p < 0.001$.
[g] Post hoc (Tukey) is as follows: β_{1a}, β_{1b}, β_{2a}, β_3, $p < 0.001$.

×25, 0.8 NA, and ×16, 0.5 NA objectives. Images were recorded with a cooled CCD camera (SPOT; Diagnostic Instruments, Stirling Heights, MI) and Metavue image processing software (Universal Imaging, Corp., West Chester, PA). Images were arranged in Adobe Photoshop 9 (Adobe Systems Inc.), and linear adjustments were performed to correct black level and contrast.

Antibodies

Primary antibodies used were as follows: rat monoclonal anti-HA (clone 3F10, 1:1,000 and 1:100 for live cell labeling; Roche Diagnostics); rabbit polyclonal anti-$Ca_V1.2$ (1:4,000; Sigma); rabbit polyclonal anti-$Ca_V2.1$ (1:2,000; Synaptic Systems); rabbit polyclonal anti-green fluorescent protein (1:20,000; Molecular Probes, Eugene, OR); mouse monoclonal anti-V5 (1:400; Invitrogen); mouse monoclonal anti-synapsin 1 (clone 46.1, 1:2,000; Synaptic Systems); rabbit polyclonal anti-synapsin 1 and 2 (1:20,000 and 1:2,000 in combination with Alexa 350; Synaptic Systems); rabbit polyclonal anti-NaChpan (1:250; Sigma); mouse monoclonal anti-β_1 (1:10,000) and anti-β_4 (1:250; both from Neuromab, Davis, CA); and rabbit polyclonal anti-β_2 (1:500; polyclonal antibody 425) and anti-β_3 (1:500; polyclonal antibody MM_2; both generous gifts from Dr. Flockerzi). Secondary antibodies used were as follows: goat anti-mouse Alexa 488 (1:2,000) and Alexa 594 (1:4,000); goat anti-rabbit Alexa 350 (1:500), Alexa 488 (1:4,000), and Alexa 594 (1:4,000); and goat anti-rat Alexa 594 (Invitrogen, 1:4,000).

Analysis

Quantification of Density and Fluorescent Intensity of $Ca_V1.2$-HA Clusters—To analyze the effects of the coexpressed β subunits on the membrane expression of $Ca_V1.2$-HA, surface fluorescence intensity was measured in 17 DIV cultured neurons as described previously (42). HA intensity values were expressed separately as percent of control for each individual experiment (transfection and culture preparation). For each condition, between 4 and 16 neurons were analyzed in each of three to seven independent experiments (culture preparations and transfections; Fig. 5*E*).

Quantification of β-V5 Fluorescent Intensity—To analyze the subcellular distribution of the heterologously expressed V5-tagged β subunits, we quantified the fluorescence intensity of the V5 stain in 13 DIV cultured hippocampal neurons. To this end, 14-bit gray scale images of the red (V5) and green (eGFP) channels of the neuron soma were acquired, and the V5 image was corrected for uneven illumination and the dark current of the camera. For each cell, a second image showing a segment of the axonal main branch at 1 mm distance from the soma was acquired and corrected accordingly. The corresponding eGFP image was used to distinguish the emerging axon from dendrites. A region of interest was manually traced around the soma, and 30-μm-long lines were placed along the proximal segments of one dendrite, the axon (representing the axon hillock), and along a distal segment of the axon 1 mm from the soma. Subsequently, the region intensities were recorded, and background was subtracted. V5 staining intensities in the dendrite, the axon hillock, and the distal axon were normalized to the soma intensity of each individual cell by calculating the dendrite/soma, distal axon/soma, and axon hillock/dendrite ratios. For each condition, between 2 and 10 neurons were analyzed in each of three to six independent experiments (culture preparations and transfections; Table 1).

Colocalization Analyses—To analyze the degree of colocalization of $Ca_V1.2$-HA and β-V5 clusters, a Z-stack of three consecutive 14-bit gray scale images (interplane distance of 0.2 μm) of the corresponding red (live cell staining of $Ca_V1.2$-HA) and green (V5) color channels were acquired using Metavue software. Next, the images were aligned and deconvolved using ImageJ software (ImageJ, National Institutes of Health, Bethesda) as described previously (45). Images were background-subtracted, and a region of interest was drawn around a dendritic segment. Colocalization was analyzed in ImageJ using two different methods: intensity correlation analysis (46) and distance-based colocalization (JACoP plugin in ImageJ; Ref. 47). Results are expressed as mean intensity correlation quotient ±95% confidence intervals and mean percentage ± 95% confidence intervals of $Ca_V1.2$-HA or β-V5 objects colocalizing with β-V5 or $Ca_V1.2$-HA, respectively. For each condition, the

indicated number of 17 DIV neurons was analyzed from two independent experiments (culture preparations and transfections; Fig. 5*B*). To determine the colocalization of endogenous β subunits with synapsin, 14-bit gray scale images of the corresponding red and green color channels were acquired using Metavue software. Subsequently images were two-dimensionally deconvolved (Metamorph) and analyzed in ImageJ using distance-based colocalization (JACoP plugin in ImageJ; Ref. 47).

Quantification of Dendritic Ca_V1.2-HA and Ca_V1.2-HA(W440A) Expression—To analyze the distribution of the overall HA fluorescence along the dendrites of 18 DIV hippocampal neurons transfected with Ca_V1.2-HA and Ca_V1.2-HA (W440A), 14-bit gray scale images of the red (HA) and green (eGFP) channel were acquired using the ×25, 0.8 NA objective. For each neuron, the HA fluorescence intensity of 2–5 dendrites was recorded along a single pixel line reaching from the soma to the distal tips of the dendrite. The corresponding eGFP image was used to distinguish dendrites from axons. The intensity values of one dendrite were normalized to the average intensity of the proximal 10 μm of the same dendrite and the moving average of 10-μm-long bins was calculated for the entire length of the dendrite. Finally, the normalized intensity values were averaged between the dendrites of one neuron. Numbers (*n*) are 23 (normal) and 25 (W440A) neurons from four separate culture preparations.

Semi-automated Analysis of eGFP and HA Fluorescent Intensity in Dendritic Spines—Analysis of dendritic spine HA and eGFP intensities in 18- and 25-DIV neurons was performed using a custom-designed Metamorph Journal (macro). Briefly, 14-bit gray scale images of the corresponding red (permeabilized staining of Ca_V1.2-HA) and green (eGFP) color channels were acquired using Metavue software. Corresponding images were aligned, and one dendritic segment of 20–50 μm length was selected for analysis. The HA and eGFP images were background-flattened and thresholded to trace fluorescent clusters (HA) and dendritic spines (eGFP) as accurately as possible. The thresholded eGFP images were transformed into a binary image, and a morphological filter (circular gradient) was applied to outline the edges of the dendritic spines. The binary and gradient images were added, and regions of interest were drawn around the dendritic spines and the dendritic shaft. Using the integrated morphometric analysis option of Metamorph, the spine size was measured in the binary eGFP image, and subsequently the regions of interest were transferred onto the HA and eGFP images to record the fluorescent intensities of each spine. Average spine intensities were background-subtracted, normalized to the average fluorescent intensity of the dendritic shaft, and finally multiplied by the respective spine size.

Statistical Analysis

Results are expressed as means ± S.E. except where otherwise indicated. Data were organized and analyzed using MS Excel and SPSS statistical software (SPSS Inc, Chicago) as indicated. Graphs and figures were generated using MS Excel, Origin 7, and Adobe Photoshop 8.0 software.

RESULTS

Cultured Hippocampal Neurons Express mRNA and Protein of All Four Ca^{2+} Channel β Subunits—It has previously been shown that the hippocampus expresses mRNA and protein of the Ca_V α_1 subunits (Ca_V1.2, Ca_V1.3, Ca_V2.1, Ca_V2.2, and Ca_V2.3), $\alpha_2\delta$ ($\alpha_2\delta$-1, $\alpha_2\delta$-2, and $\alpha_2\delta$-3), and of all four β subunits (12–15, 21, 23). Still, little is known about the subcellular distribution of β subunits in neurons and about the specific subunit composition of Ca_V complexes in pre- and postsynaptic compartments. Therefore, we addressed the following three questions. 1) Which of the β subunits are expressed in a defined neuronal culture system, low density hippocampal neurons? 2) Are these β subunits differentially distributed within hippocampal neurons? 3) Do their colocalization and functional interactions reveal evidence for preferred interaction partners of specific α_1 subunits?

Employing quantitative TaqMan RT-PCR analysis, we determined whether and how much mRNA of the four β subunits is expressed in hippocampus tissue of 2-week-old BALB/c mice and in cultured hippocampal neurons (40, 41).[4] In hippocampus, we detected similar expression levels of all β subunit isoforms. The mRNA levels of β_2 and β_4 were slightly but not significantly higher than those of β_1 and β_3 (Fig. 1*A*, *left*). Finding all four β subunits expressed in mouse hippocampus was not surprising considering the cellular heterogeneity of the hippocampal formation. Remarkably, however, mRNA of all four β subunits was also expressed in low density cultured hippocampal neurons (Fig. 1*A*, *right*), which consist of ~90% glutamatergic pyramidal cells (37, 48).

Because quantitative RT-PCR analysis revealed the expression of all four β subunits in the cultured neurons, we next investigated their subcellular distribution using immunofluorescence labeling with antibodies specific for the individual β isoforms (Fig. 1*B*; supplemental Fig. 1). All four β isoforms could be detected in the soma and in the dendrites. Higher magnification micrographs of dendritic segments (Fig. 1*B*, *lower panel*) revealed a delicate punctate staining pattern of all isoforms along the dendritic shaft (*arrows*) and adjacent to the shaft in positions typical for dendritic spines (*open arrowheads*). Double immunofluorescence labeling with an antibody against synapsin, marking the presynaptic vesicle compartment (50), showed that some of the β clusters overlapped or colocalized with synapsin (Fig. 1*B*, *solid arrowheads*). β_1 clusters were primarily located adjacent to synapsin clusters, whereas a subset of β_2 and β_4 clusters was colocalized with synapsin (*yellow* in Fig. 1*B*). Partial overlap of all β subunits with synapsin was further supported by object-based colocalization analysis of 24 DIV neurons (% of β clusters colocalized with synapsin ± 95% confidence intervals (*n*): β_1, 46 ± 4 (21); β_2, 48 ± 4 (22); β_3, 42 ± 4 (23); β_4, 45 ± 5 (22); ANOVA, $F_{(3,84)} = 1.64$; $p = 0.19$). Here, the preferential colocalizations of β_2 and β_4 observed in the qualitative analysis were not detected, mainly because of the large abundance of extrasynaptic β clusters along the dendritic shaft.

The localization of β subunits along the dendritic shaft and at synaptic sites suggests their association with postsynaptic and presynaptic Ca_V α_1 subunits, respectively. For example, the

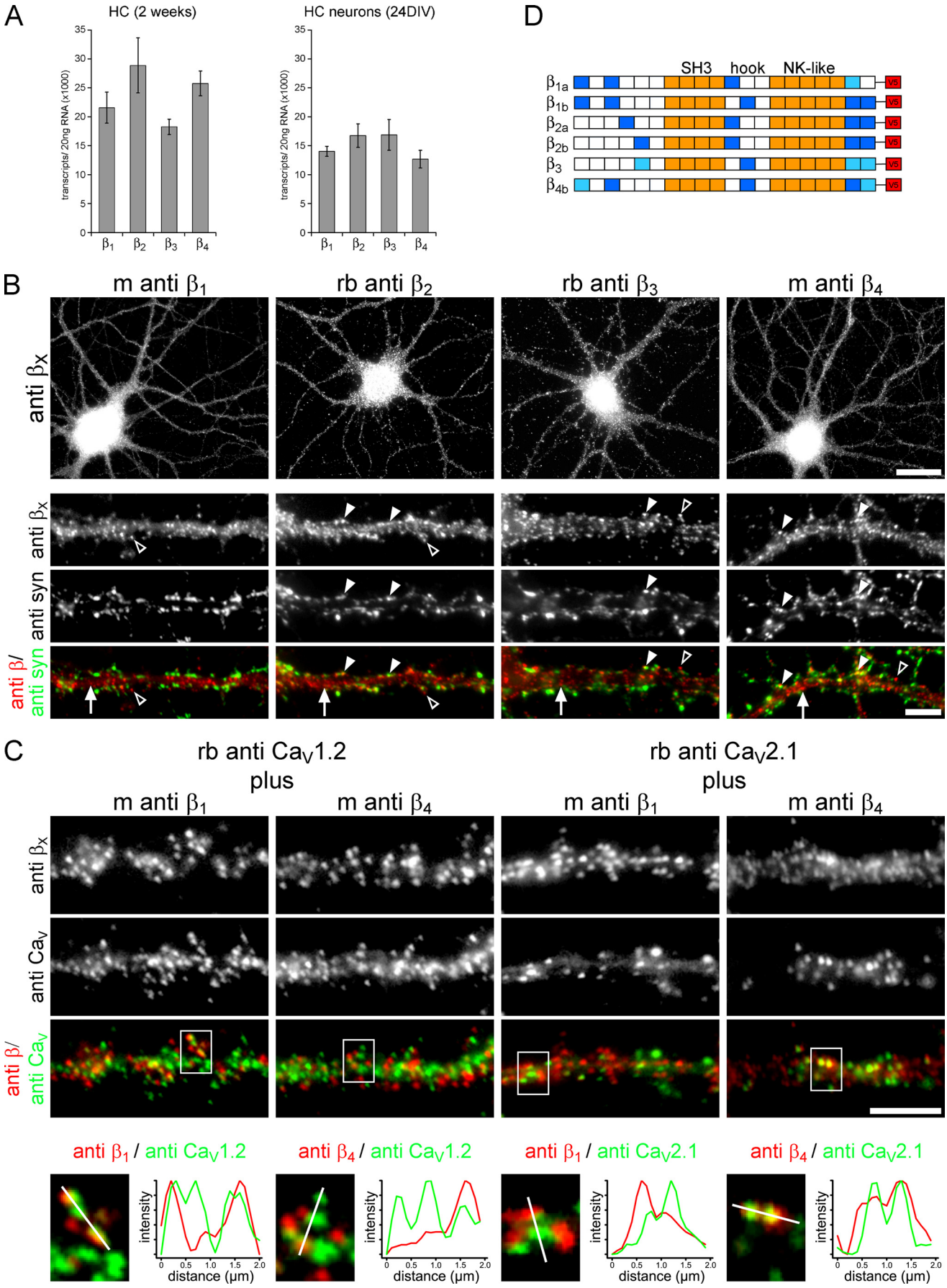
A
HC (2 weeks)
HC neurons (24DIV)
transcripts/ 20ng RNA (x1000)
β1 β2 β3 β4
D
SH3 hook NK-like
β1a β1b β2a β2b β3 β4b
V5
B
m anti β1
rb anti β2
rb anti β3
m anti β4
anti βx
anti syn
anti β/ anti syn
C
rb anti CaV1.2 plus
rb anti CaV2.1 plus
anti Cav
anti β/ anti Cav
anti β1 / anti CaV1.2
anti β4 / anti CaV1.2
anti β1 / anti CaV2.1
anti β4 / anti CaV2.1
intensity
distance (μm)

overall β subunit distribution along the dendrites was strikingly similar to the localization of endogenous L-type $Ca_V1.2$ (15) and $Ca_V1.2$-HA expressed in the membrane (15, 42, 49). Thus, we next investigated whether β_1 and β_4 subunits specifically colocalize with postsynaptic ($Ca_V1.2$) or presynaptic ($Ca_V2.1$) α_1 subunits. Double immunofluorescence demonstrated that a subset of $Ca_V1.2$ clusters was precisely colocalized with β_1 clusters, especially in positions typical for dendritic spines. In contrast, the overlap of $Ca_V1.2$ and β_4 clusters along the dendritic shaft seemed to be largely random (Fig. 1*C*, *left*). This observation was further supported by line scan analysis of selected regions (Fig. 1*C*, *lower panel*). On the other hand, a subset of β_4 clusters was precisely colocalized with $Ca_V2.1$ clusters, whereas β_1 clusters were only loosely associated with this presynaptic α_1 subunit (Fig. 1*C*, *right*). The inherent inability to distinguish membrane-expressed channel clusters from intracellular pools and inevitable differences in the quality of the antibodies prevented the quantitative analysis of the colocalization. Together, this emphasizes the need for a standardized method for investigating β subunit localization and the importance to specifically identify and analyze membrane-expressed channels.

Six Different V5-tagged β Subunits Show a Similar Distribution Pattern in the Somatodendritic Compartment of Cultured Hippocampal Neurons—Therefore, we tagged β_{1a}, β_{1b}, β_{2a}, β_{2b}, β_3, and β_{4b} with a C-terminal V5 tag (Fig. 1*D*) and expressed them together with soluble eGFP or an extracellular HA-tagged $Ca_V1.2$ in the low density cultured hippocampal neurons. This approach has the advantage of localizing all examined β subunits with the same antibody and of investigating their colocalization exclusively with the population of membrane-expressed Ca_V channels. Furthermore, it allowed us to extend the analysis to additional β splice variants for which no specific antibodies are available. The eGFP fluorescence enabled us to independently assess the quality of the transfected neurons and to unambiguously identify neuronal compartments such as axons with presynaptic boutons (*e.g.* Figs. 3 and 4) and dendrites with dendritic spines (*e.g.* Fig. 2*B*). To obtain similar expression levels, the amounts of DNA of all transfected β constructs were titrated between 0.5 and 2 μg of DNA per 60-mm culture dish. To exclude interference of elevated expression levels on the distribution pattern, we analyzed exclusively medium to low expressing neurons.

As already suggested by the antibody labeling of the endogenous β subunits (Fig. 1*B*), all recombinant β subunit constructs also displayed very similar overall distribution patterns (Fig. 2*A*). All analyzed isoforms and splice variants were expressed in the somatodendritic compartment as well as in the axons (Fig. 2*A*, *arrows*). In dendrites, all β-V5 constructs were distributed in a punctate and discretely clustered pattern along the dendritic shaft and also in the dendritic spines (Fig. 2*B*, *arrowheads*). This distribution pattern and the apparent density of the β clusters was similar to the staining pattern of the endogenous β subunits (Fig. 1*B*). Moreover, analysis of the dendrite-over-soma ratio of the fluorescence intensity (Table 1) demonstrated that, with the exception of the β_{2a} isoform, all β subunits had a similar expression density in the dendrites. The higher expression of the β_{2a} isoform was the result of its accumulation at the membrane due to N-terminal palmitoylation (51, 52); mutation of the palmitoylation site, the cysteines at positions 3 and 4 to serines, abolished this effect (Table 1).

Isoform-specific Localization of β-V5 Subunits in the Distal Axon—Because all β-V5 subunits were able to enter the axonal compartment (Fig. 2*A*), we next sought to analyze their expression pattern in the distal axon. To this end, we followed the main axonal branch of the transfected neuron for 1 mm (based on the eGFP stain; Fig. 3*A*) and analyzed the axon-over-soma ratio of V5 intensity separately for each individual neuron (Table 1). Axonal expression of all β-V5 constructs was evident as fine puncta along the axon (Fig. 3*A*). The expression levels of both β_1 splice variants (β_{1a} and β_{1b}) were significantly lower compared with the other β subunits (Fig. 3*A*; Table 1). This reduced targeting of β_1 subunits into the distal axon evidently did not depend on the expression levels of individual neurons. First, this differential distribution pattern was observed in neurons displaying a wide range of expression levels; and second, β_1-expressing neurons showed the same somatic β-V5 intensity as neurons expressing the other βs (ANOVA, $F_{(6,152)} = 2.16$; $p = 0.18$). The difference in axonal targeting was especially apparent when β_{1b}-V5 was coexpressed together with a C-terminally green fluorescent protein-tagged β_{4b} subunit in the same hippocampal neuron (Fig. 3*B*). Both β subunits labeled the soma and the dendrites, including the most distal tips of the dendrites, to a similar degree. In contrast, the axonal localization of β_{1b}-V5 was restricted to the proximal segments, whereas β_{4b}-green fluorescent protein label was intense throughout all the axonal branches (Fig. 3*B*, *color overlay*). Thus, β subunits display an isoform-specific expression in the axonal compartment in that β_2, β_3, and β_4

FIGURE 1. **mRNA expression and immunocytochemical localization of all four Ca^{2+} channel β subunit isoforms in cultured mouse hippocampal neurons.** *A,* TaqMan RT-PCR expression profile of the four Ca^{2+} channel β subunits in hippocampi from 2-week-old mice (*HC*, *left*) and cultured mouse hippocampal neurons (*HC* neurons, *right*) differentiated 24 DIV. In hippocampus, β_2 and β_4 isoforms are expressed at slightly but not significantly higher levels than β_1 and β_3 (ANOVA, $F_{(3,8)} = 2.42$; $p = 0.14$). Cultured hippocampal neurons express all β isoforms at similar levels (ANOVA, $F_{(3,16)} = 1.20$; $p = 0.34$). *n*, 3 tissue and 5 culture preparations; data are presented as mean number of transcripts per 20 ng of RNA ± S.E. *B,* representative cultured hippocampal neurons (20 DIV) labeled with mouse monoclonal (*m*; β_1 and β_4) or rabbit polyclonal (*rb*; β_2 and β_3) antibodies show a similar expression and distribution pattern of all four endogenous β subunits in the soma and dendrites. Contrast in micrographs is optimized to visualize the weak labeling on the dendrites; therefore, the staining in the somata appears saturated. Dendrite segments of all βs shown at higher magnifications (*lower panel*) reveal a similar punctate staining pattern along the dendritic shafts (*red, arrows*) and adjacent to the shafts in dendritic spines (*open arrowheads*). β_2, β_3, and β_4 puncta partially overlap or colocalize with the presynaptic marker synapsin (*yellow, solid arrowheads*). *C,* double immunofluorescence labeling and line scan analyses of mouse monoclonal (*m*) β_1 and β_4 antibodies together with rabbit polyclonal (*rb*) anti-$Ca_V1.2$ (*left*) and anti-$Ca_V2.1$ (*right*) antibodies in 24 DIV cultured neurons. A subset of $Ca_V1.2$ clusters colocalizes with β_1 along the dendritic shaft and in dendritic spines (line scan analysis, *lower panel*), whereas association with β_4 is less pronounced. In contrast, presynaptic $Ca_V2.1$ clusters colocalize with β_4 but rarely with β_1 clusters. *D,* comparative exon structures of all C-terminal V5-tagged β subunit isoforms and splice variants used in this study. Exon similarities of the β_1, β_3, and β_4 genes were identified in the mouse genome (NCBI m37 assembly) in relation to the overall structure of the β_2 gene (30, 31). Color codes: *orange*, conserved exons in the Src homology 3 and guanylate kinase-like domain; *blue*, high sequence similarity; *light blue*, lower sequence similarity. *Scale bars,* 25 and 5 μm (*B*) and 5 μm (*C*).

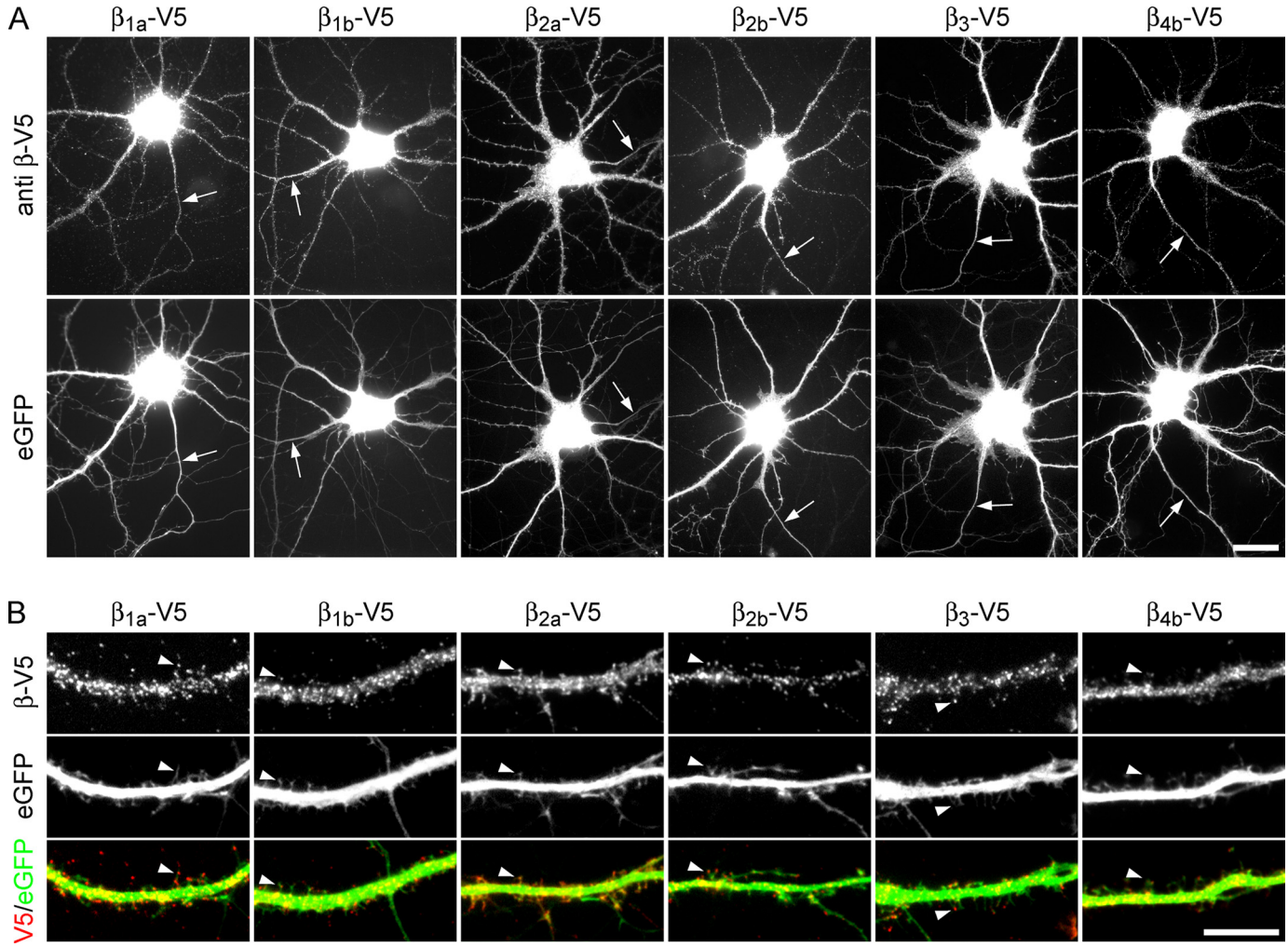

FIGURE 2. **Somatodendritic distribution pattern of six V5-tagged β subunit isoforms and splice variants in cultured hippocampal neurons.** Cultured hippocampal neurons (2 weeks old) were transfected with different β-V5 constructs together with eGFP and labeled with an antibody against the C-terminal V5 epitope. *A,* immunostaining reveals a similar expression of all V5-tagged β subunits in the soma, the dendrites, and in the proximal regions of the axon (*arrows*). The axon was identified based on its characteristic appearance in the eGFP image (*lower panel*). To visualize the weak staining in the smaller dendrites and axons, the contrast of the images was enhanced, and thus the staining of the cell soma appears saturated. *B,* details of dendritic segments; all β-V5 subunits display a punctate, clustered distribution pattern along the dendritic shaft. In addition all β subunits are localized in small clusters in the dendritic spines (*arrowheads*) identified in the eGFP image. Note that the palmitoylated β_{2a} isoform also shows a diffuse staining of the membrane. *Scale bars,* 25 μm (*A*) and 10 μm (*B*).

isoforms are expressed throughout the axon, whereas β_{1a} and β_{1b} are largely excluded from the distal axon and small axonal branches.

All β Subunit Isoforms Can Accumulate in the Presynaptic Compartment—As all β subunits were able to enter the axon, although to different degrees, it was important to examine whether they also accumulate in the presynaptic compartment. To this end, presynaptic terminals were identified by the eGFP label and by concomitant immunostaining with an antibody against synapsin (Fig. 4) or the vesicular glutamate transporter (vGlut1, data not shown). Where axons of transfected neurons made contacts with nontransfected postsynaptic neurons, clusters of V5-labeled β subunits were unambiguously identified as presynaptic. In triple-labeling experiments, we regularly observed clusters of all six examined β isoforms and splice variants colocalized with synapsin clusters in transfected eGFP-positive axons (Fig. 4, *anti-V5 label* and *color overlay*). This synaptic localization was repeatedly observed in both *en passant* boutons (Fig. 4, β_{1a}*-V5*, β_{1b}*-V5*, β_3*-V5*) and in terminal synapses (β_{2a}-V5, β_{2b}*-V5*, and β_{4b}*-V5*) for all the V5-tagged β subunits. Thus, even in those cases where only a limited amount of β was expressed in the distal axon (β_{1a} and β_{1b}), the β subunits could specifically accumulate in the synapse; presumably due to their association with presynaptic Ca_Vs.

All β Subunit Isoforms Can Interact with the Postsynaptic L-type Channel $Ca_V1.2$—A colocalization of β subunits with presynaptic marker proteins is indicative of their association with presynaptic Ca_V complexes. Likewise, the punctate distribution of the βs in the somatodendritic compartment (*cf.* Fig. 1*B* and Fig. 2) is suggestive for their association with postsynaptic Ca_Vs. $Ca_V1.2$ is the only postsynaptic L-type channel whose precise subcellular localization on the soma, dendrites, and dendritic spines of cultured hippocampal neurons is known (15). Therefore, we coexpressed the V5-tagged β subunits together with the external epitope-tagged $Ca_V1.2$-HA to analyze β subunit interaction with

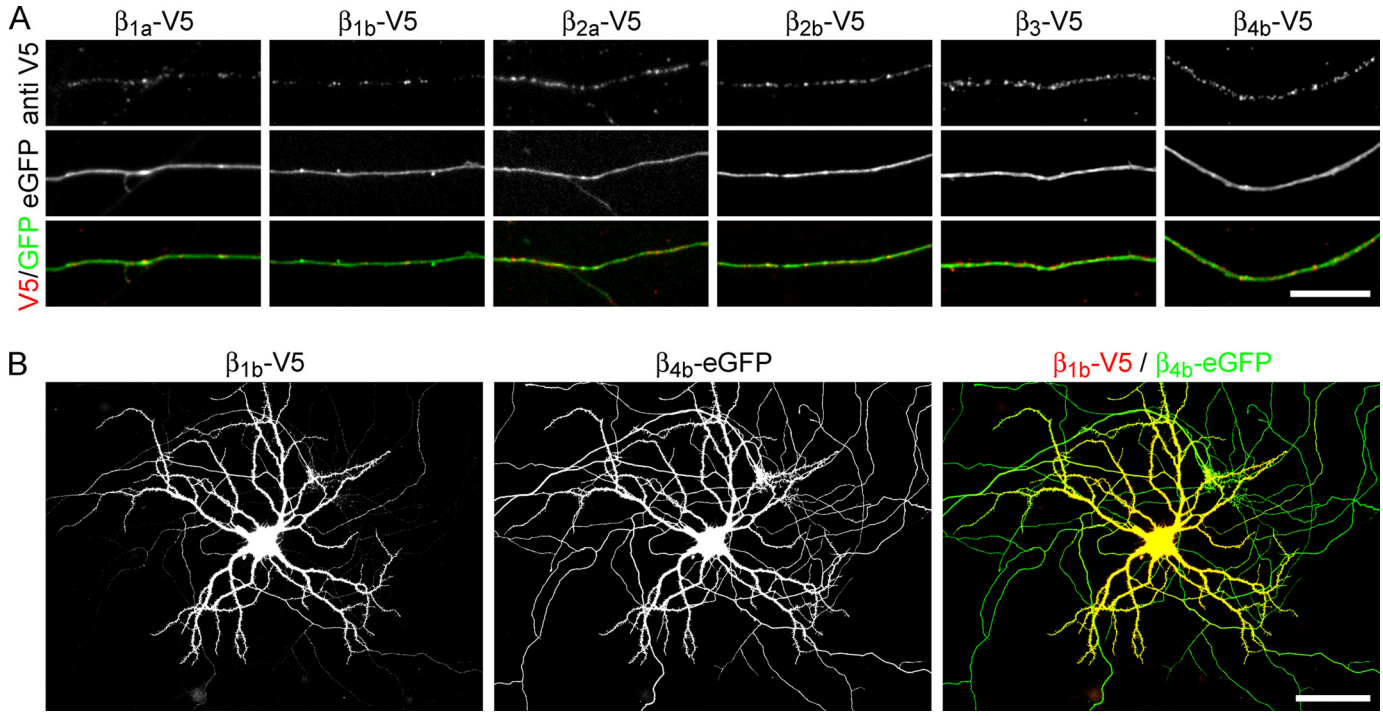

FIGURE 3. **Isoform-specific localization of V5-tagged β subunits in the distal axon of cultured hippocampal neurons.** *A,* all examined β-V5 subunit isoforms display a clustered staining pattern along the axonal main branch of 2-week-old cultured hippocampal neurons at ~1 mm distance from the soma. The intensity and frequency of axonal clusters are much lower for β_{1a} and β_{1b} compared with the other β subunits (for quantification see Table 1). *B,* representative cultured hippocampal neuron (17 DIV) cotransfected with β_{1b}-V5 and β_{4b}-eGFP and double-labeled with anti-V5 and anti-GFP antibodies. The distribution of β_{1b}-V5 is confined to the somatodendritic compartment and the proximal regions of the axon (*left, yellow* in the *color overlay*), whereas β_{4b}-eGFP expression is similarly high throughout the axon and the axonal branches (*middle, green* in the *color overlay*). *Scale bars,* 10 μm (*A*) and 25 μm (*B*).

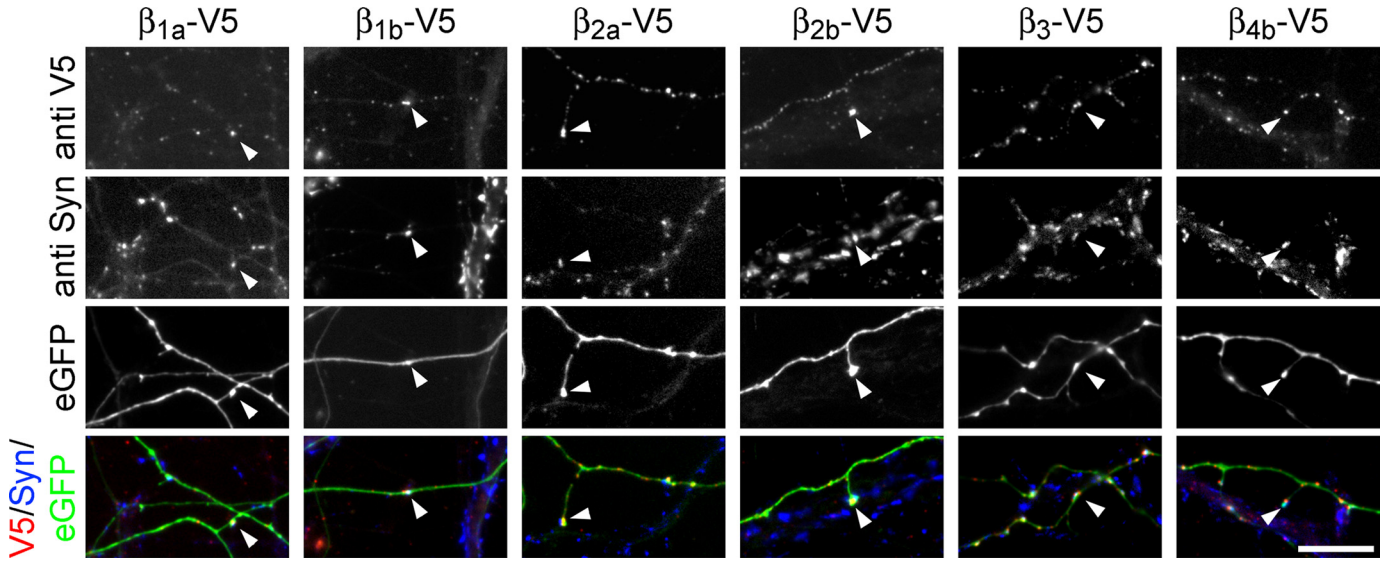

FIGURE 4. **Localization of β-V5 subunits in the presynaptic compartment of cultured hippocampal neurons.** Representative axonal segments of triple-labeled 17–20 DIV hippocampal neurons were transfected with different β-V5 constructs and eGFP (postsynaptic nontransfected neurons are not stained). eGFP fluorescence allows to morphologically identify axons with their varicosities typical for *en passant* synapses (examples in β_{1a}-V5, β_{1b}-V5, and β_3-V5) and short axonal branches with presynaptic terminals (examples in β_{2a}-V5, β_{2b}-V5, and β_{4b}-V5). Double immunostaining with an antibody against synapsin (anti-Syn) identifies these axonal varicosities and terminals as presynaptic compartments. All six V5-tagged β subunit isoforms (anti-V5) were found to accumulate in presynaptic terminals as based on their colocalization with synapsin (anti-Syn) and eGFP (examples indicated by *arrowheads*). Presynaptic accumulation was observed repeatedly for all isoforms in 3–12 analyzed cells of at least two independent experiments. *Scale bar,* 10 μm.

postsynaptic Ca_Vs. As described previously, live cell staining using an anti-HA antibody revealed the localization of the membrane-expressed $Ca_V1.2$-HA in small clusters on the shafts of the dendrites and in the dendritic spines (Fig. 5*A*) at a density of 1–2 clusters/μm (15, 42). Subsequent fixation and permeabilization of the live cell-labeled neurons allows us to immunostain the intracellular β subunits in addition. Such double staining clearly showed that clusters of membrane-incorporated $Ca_V1.2$-HA are colocalized with each one of the coexpressed β subunits (Fig. 5*A*), indicating the association of all of the examined β isoforms with $Ca_V1.2$-HA in the postsynaptic compartment.

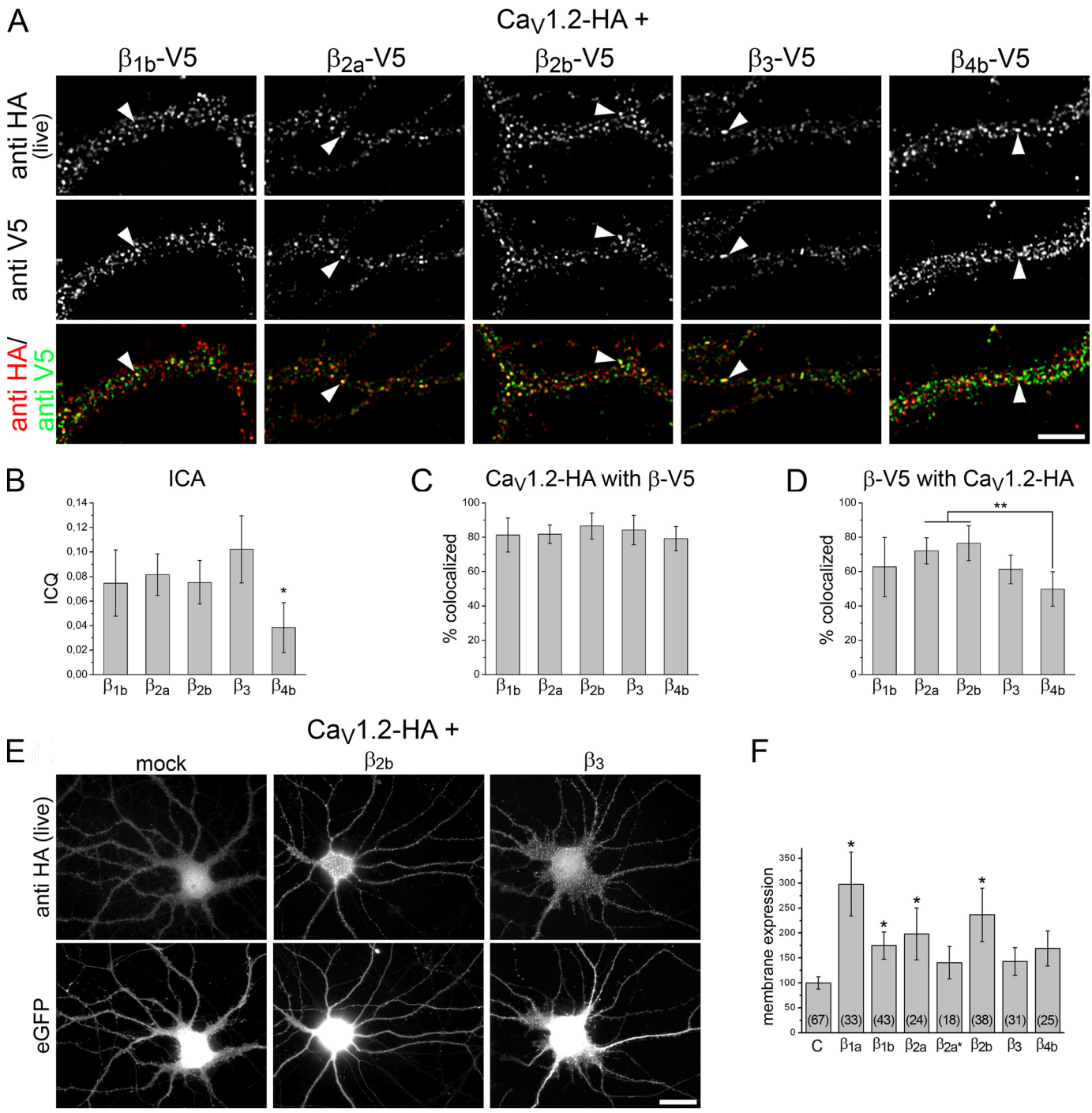

FIGURE 5. **Colocalization of β-V5 subunits with membrane-expressed Ca_V1.2-HA in dendrites of cultured hippocampal neurons.** *A,* dendritic segments of hippocampal neurons (18 DIV), transfected with Ca_V1.2-HA and a V5-tagged β subunit, labeled with an antibody against the extracellular HA epitope prior to fixation (anti-HA, live) and with anti-V5 after subsequent permeabilization. Clusters of all β subunits were colocalized with the membrane-expressed Ca_V1.2-HA (examples indicated by *arrowheads*; *yellow* in *color overlay*). *B*, intensity correlation analysis (*ICA*) of α_1-β colocalization reveals a similar intensity correlation coefficient (*ICQ*) for all coexpressed β subunits with the exception of β_{4b}, for which it was significantly reduced. ANOVA, $F_{(4,54)} = 5.88$; $p = 0.001$. *C,* object-based colocalization shows that ~80% of Ca_V1.2-HA clusters are colocalized with the cotransfected β subunit independent of the respective isotype. ANOVA, $F_{(4,54)} = 0.76$; $p = 0.56$. *D,* conversely, ~50–75% of β-V5 clusters are colocalized with Ca_V1.2-HA clusters. Interestingly, again the colocalization with β_{4b} was reduced when compared with β_{2a} and β_{2b} ($p = 0.002$ and 0.001, respectively). ANOVA, $F_{(4,54)} = 5.81$; $p = 0.001$ and Tukey post hoc analysis. *E,* coexpression of Ca_V1.2-HA with different β subunit isoforms and splice variants (example images of β_{2b} and β_3) results in a strong increase in Ca_V1.2-HA membrane expression compared with control cells (mock-transfected). *F,* quantification of surface HA staining intensity reveals a significant effect of the β_1 and β_2 isoforms on surface expression of Ca_V1.2-HA, compared with mock-transfected control (*c*) neurons. ANOVA, $F_{(7,271)} = 12.78$; $p < 0.0001$; Tukey post hoc analysis, $p < 0.001$ (β_{1a}), $p = 0.014$ (β_{1b}), $p = 0.005$ (β_{2a}), $p = 0.86$ (β_{2a}* = β_{2a}-SS) $p < 0.001$ (β_{2b}), $p = 0.623$ (β_3), and $p = 0.134$ (β_{4b}). *Scale bars,* 10 μm (*A*) and 25 μm (*E*); *error bars* indicate 95% confidence intervals.

To reveal potential differences in the degree of α_1-β colocalization, we further analyzed the images by two independent quantification methods, intensity correlation analysis (46) and object-based colocalization (47). Intensity correlation analysis (Fig. 5*B*) showed similar degrees of colocalization for all β subunits except for β_{4b}, for which the intensity correlation quo-

tient was slightly but significantly reduced. Object-based colocalization supported the initial visual observation by demonstrating that the vast majority of the membrane-expressed $Ca_V1.2$-HA clusters (~80%) was colocalized with each of the coexpressed β subunit isoforms (Fig. 5*C*). Conversely, between ~50 and 75% of the β subunit clusters colocalized with membrane-expressed $Ca_V1.2$-HA. Interestingly, also in this analysis the β_{4b} showed the lowest degree of colocalization (Fig. 5*D*). Together, these analyses demonstrate that in cultured hippocampal neurons clusters of postsynaptic $Ca_V1.2$ channels are almost fully occupied by each of the β isoforms and splice variants. However, clusters of β subunits also exist independently of the $Ca_V1.2$-HA clusters, and this is most evident in the case of the β_{4b} isoform.

In contrast to other Ca_V targeting studies, we routinely express the α_1 subunit without auxiliary $\alpha_2\delta$ and β subunits in cultured hippocampal neurons (15, 42, 49). As a consequence, subcellular localization, targeting, and membrane expression of these expressed subunits entirely depend on the interaction of the heterologous channel with endogenous β and $\alpha_2\delta$ subunits. This minimizes possible effects of overexpression on the subcellular localization. To test whether the amount of β subunits is limiting for membrane expression of $Ca_V1.2$, we analyzed the intensity of $Ca_V1.2$-HA surface expression upon coexpression of the different β subunits. As control, we coexpressed a plasmid bearing the same promoter but no coding sequence together with $Ca_V1.2$-HA (Fig. 5*E*, *mock*). Coexpression of all β-V5 subunits resulted in a substantial increase of the membrane expression of $Ca_V1.2$-HA up to 300% (β_{1a}) of controls without a β (Fig. 5, *E* and *F*). This suggests that also in neurons, the amount of membrane-expressed Ca_V α_1 subunits is limited by the amount of available β subunits. Interestingly, with the β_{1a}, β_{1b}, and β_{2a} isoforms, the increase in membrane expression of $Ca_V1.2$-HA was larger and statistically significant compared with that with β_3, β_{4b}, and the nonpalmitoylated β_{2a} mutant. This observation indicates that β subunits enhance membrane expression in an isoform-specific manner.

Intact α_1-β Subunit Interaction at the AID Is Essential for Neuronal Membrane Expression of $Ca_V1.2$-HA—Studies in heterologous expression systems have demonstrated the requirement of α_1-β interactions for functional membrane expression of the Ca_V complex (reviewed in Ref. 31). Recently, the mutation of a key tryptophan in the AID (53) of the intracellular I–II linker of $Ca_V2.2$ has been shown to strongly reduce surface expression of the channel in human embryonic kidney cells (54). To determine the role of α_1-β interactions for membrane expression of the α_1 subunit and for the targeting of the β subunit in a native neuronal cell type, we mutated the analogous tryptophan in the AID of the $Ca_V1.2$-HA to alanine (W440A). Live cell staining of normal $Ca_V1.2$-HA showed the typical clustered membrane expression pattern (Fig. 6*A*, anti-HA, *left*; n = 56 neurons from seven independent culture preparations and transfections). In contrast, the mutated channel $Ca_V1.2$-HA(W440A) was not detectable on the surface of cultured hippocampal neurons in live cell staining experiments (Fig. 6*A*, *anti-HA, right*) in all neurons analyzed (n = 54 neurons from seven independent culture preparations and transfections). This was not due to an overall failure of protein expression, because subsequent permeabilization and immunolabeling with an antibody against $Ca_V1.2$ revealed the presence of similar amounts of normal and W440A mutant channel protein in the transfected cells (Fig. 6*A*, *anti-$Ca_V1.2$*).

To test whether an excess of β subunits, which should enable β subunits to occupy even low affinity interaction sites (55), might at least partially rescue the loss of membrane expression in the W440A mutant, we coexpressed the different β isoforms with $Ca_V1.2$-HA and $Ca_V1.2$-HA(W440A) (supplemental Fig. 2). Whereas increased membrane expression of the $Ca_V1.2$-HA was observed with all the β subunits, none of the β subunits induced a detectable membrane expression of $Ca_V1.2$-HA(W440A), suggesting an exclusive and essential role of the α_1-β interaction at the AID for neuronal membrane expression.

In principle, the failure in membrane expression of $Ca_V1.2$-HA(W440A) could also be explained by a compromised trafficking of the mutated channel into the distal parts of the dendritic tree. Thus, we analyzed the distribution of the overall fluorescence signal in the dendrites of permeabilized neurons transfected with normal and mutated $Ca_V1.2$-HA. The HA labeling intensity in the proximal dendrite was indistinguishable between normal and the W440A mutant channels ($t_{(45)}$ = −0.04; p = 0.96; n, normal, 22; W440A, 25). Analysis of the relative decrease in fluorescence (Fig. 6*B*) showed a very similar rate of decrease of $Ca_V1.2$-HA and $Ca_V1.2$-HA(W440A) expression along the dendrites; and even in the most distal regions of the dendrites (~250 μm) HA labeling of the W440A mutant was robust. The small reduction in the total HA fluorescence in $Ca_V1.2$-HA(W440A) compared with the normal channel along the entire length of the dendrite is likely the effect of the missing membrane fraction of the HA staining (Fig. 6*B*). Thus, mutation of AID-β interactions did not reduce expression levels nor the overall targeting of the $Ca_V1.2$(W440A) throughout the dendritic tree, but it specifically disrupted the membrane expression of the channel.

Intact α_1-β Subunit Interaction at the AID Is Essential for Dendritic Spine Targeting of $Ca_V1.2$-HA—A hallmark of the subcellular distribution of $Ca_V1.2$ is its clustered localization in the heads and necks of dendritic spines close to but not necessarily within the postsynaptic density (15, 42). Therefore, we next investigated the importance of the functional α_1-β interaction for the characteristic localization of $Ca_V1.2$ channel complexes in dendritic spines. The localization of $Ca_V1.2$-HA in the membrane of dendritic spines is most strikingly revealed by live cell labeling of the extracellular HA epitope (15, 42). Nevertheless, also in fixed and permeabilized neurons, the clusters in dendritic spines are discernible from the HA stain in the dendritic shaft, which represents both the membrane fraction and the intracellular pool of $Ca_V1.2$-HA (Fig. 6*C*, 18 and 25 DIV, normal). At 18 DIV, the majority of spines are long and filopodia-like, and accordingly $Ca_V1.2$-HA clusters are spread out over a fair distance from the shaft. At 25 DIV, many spines assumed a mature mushroom-like shape, leading to a more regular alignment of $Ca_V1.2$-HA clusters at both sides of the dendritic shaft. In contrast, in permeabilized neurons transfected with $Ca_V1.2$-HA(W440A), dendritic spines were devoid of HA immunolabel, both at 18 and 25 DIV (Fig. 6*C*, *W440A*). The

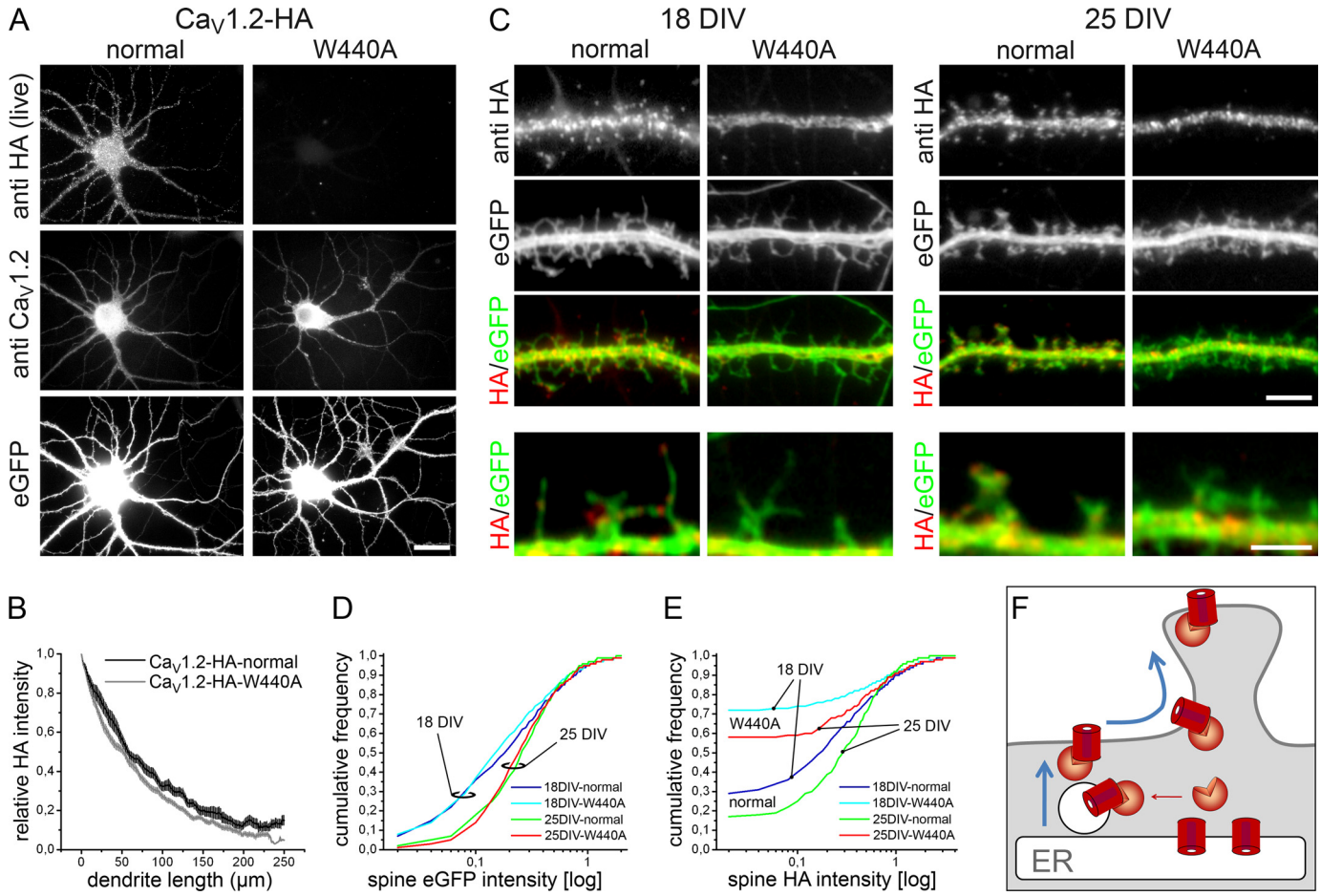

FIGURE 6. **Mutation of an essential residue of the AID (W440A) of $Ca_V1.2$ prevents neuronal membrane expression and dendritic spine targeting of $Ca_V1.2$-HA.** *A,* representative cultured hippocampal neurons (17 DIV) transfected with $Ca_V1.2$-HA (normal) or the W440A mutant (W440A) labeled with an antibody against the extracellular HA epitope prior to fixation (anti-HA, live) and with anti-$Ca_V1.2$ after permeabilization. Surface expression (anti-HA, live) of $Ca_V1.2$-HA(W440A) is completely missing, although expression of total $Ca_V1.2$ protein (anti-$Ca_V1.2$) was similar for $Ca_V1.2$-HA and W440A. Comparable neurons were selected based on the expression of cotransfected eGFP (*eGFP*). *B,* quantification of total fluorescence intensity (anti-HA in permeabilized cells) shows a similar expression of $Ca_V1.2$-HA and $Ca_V1.2$-HA(W440A) throughout the entire length of the dendrites of 18 DIV hippocampal neurons. *Error bars* represent ± S.E. *n*, 23 (normal) and 25 (W440A) neurons from four separate culture preparations. *C,* dendritic segments of 18 and 25 DIV neurons transfected with normal or W440A $Ca_V1.2$-HA plus eGFP. Neurons were immunolabeled with anti-HA after pF fixation and permeabilization. Similar to live-stained neurons, $Ca_V1.2$-HA is localized in small clusters in the dendritic shaft and spines. In contrast, $Ca_V1.2$-HA(W440A) label is restricted to the shaft, and clusters are missing. eGFP reveals filopodia-like spines at 18 DIV and mushroom-shaped spines at 25 DIV. Magnified *color overlays* of anti-HA (*green/yellow*) and eGFP (*green*) demonstrate the presence of $Ca_V1.2$-HA clusters and the absence of $Ca_V1.2$-HA(W440A) staining in both types of spines. *D*, plotting the cumulative frequency of total eGFP intensity per dendritic spine (arbitrary units) shows that dendritic spine sizes are not different in neurons transfected with $Ca_V1.2$-HA or W440A, although many spines are larger in 25 DIV (*red* and *green lines*) compared with 18 DIV neurons (*light blue* and *blue lines*). *E,* cumulative frequency distribution of total HA intensity per dendritic spine demonstrates that in neurons expressing $Ca_V1.2$-HA(W440A) ~60–70% of the spines are devoid of HA staining (*red* and *light blue lines*), whereas the vast majority of spines express $Ca_V1.2$-HA (only ~20–30% without HA stain, *green* and *blue lines*). *F,* model of $Ca_V1.2$ targeting into dendritic spines. Cytoplasmic membrane systems containing $Ca_V1.2$ are confined to the dendritic shaft. Association of a β subunit promotes the insertion of the channel into the dendritic membrane. Channel complexes enter the spine by lateral diffusion in the membrane. *Scale bars*, 25 µm (*A*) and 5 and 2.5 µm (*C*).

immunolabel of the W440A mutant channel was restricted to the dendritic shafts, where it also lacked the clustered appearance of the membrane-incorporated channels. Thus, the lack of membrane incorporation of the W440A mutant Ca^{2+} channel revealed that cytoplasmic membrane organelles containing the α_1 subunits are absent from dendritic spines.

The lack of W440A label from the spines was observed in both immature filopodia-like spines at 18 DIV and in mature mushroom-like spines in 25 DIV cultured neurons (magnified micrographs in Fig. 6*C*). Semi-automated analysis (see under "Experimental Procedures") of the dendritic spine size based on the eGFP intensity revealed a significant increase of the average spine volume between 18 and 25 DIV neurons (eGFP intensity (arbitrary units ± S.E.) 18 DIV, 0.30 ± 0.01; 25 DIV, 0.34 ± 0.01; $t_{(2376)} = 2.53$, $p = 0.011$). However, at both time points, the mean spine volumes (Table 2) and spine volume distributions (Fig. 6*D*) were indistinguishable between neurons transfected with the normal and the W440A mutant $Ca_V1.2$-HA. Moreover, the overall shape and density of spines were similar in both conditions (Fig. 6*C*; quantitation not shown). This indicates that the absence of $Ca_V1.2$-HA(W440A) label from spines did not result from potential deficits in the maturation of spines when the neurons were transfected with the mutant channel.

Analysis of the dendritic spine HA intensity revealed a dramatic difference between neurons transfected with normal $Ca_V1.2$-HA or with W440A (Table 2). This difference is clearly reflected in the cumulative frequency distribution diagram of the spine HA intensities (Fig. 6*E*). Plotting the relative frequen-

TABLE 2

Analysis of channel expression (HA intensity) in anti-HA-immunolabeled fixed/permeabilized neurons transfected with $Ca_V1.2$-HA or with $Ca_V1.2$-HA(W440A) compared with dendritic spine volume (eGFP intensity)

Number of spines (neurons) analyzed were as follows: 18 DIV, $Ca_V1.2$-HA, 852 (24) and $Ca_V1.2$-HA(W440A), 768 (24), from four independent culture preparations; 25 DIV, $Ca_V1.2$-HA, 359 (9) and $Ca_V1.2$-HA(W440A), 399 (9), from two independent culture preparations.

	DIV	$Ca_V1.2$-HA, mean ± S.E. (median)	$Ca_V1.2$-HA(W440A), mean ± S.E. (median)	Statistic	*p*
HA	18	0.39 ± 0.02 (0.17)[a]	0.27 ± 0.03 (0.00)	$Z = -13.80$[b]	$p \ll 0.001$
	25	0.39 ± 0.02 (0.29)	0.32 ± 0.04 (0.00)	$Z = -8.12$[b]	$p \ll 0.001$
eGFP	18	0.31 ± 0.01 (0.18)	0.29 ± 0.01 (0.15)	$t_{(1618)} = 1.05$[c]	0.29
	25	0.33 ± 0.01 (0.26)	0.35 ± 0.02 (0.24)	$t_{(756)} = 0.83$[c]	0.41

[a] Intensity is shown in arbitrary units (total spine gray scale intensity).
[b] Mann-Whitney U test was used.
[c] *t* test was used.

cies of the individual recorded spine HA intensities against their intensity values indicated that the reduced overall mean fluorescence values in spines of neurons transfected with $Ca_V1.2$-HA(W440A) were due to the greatly increased population of spines containing no HA staining at all. Whereas with $Ca_V1.2$-HA only 29% (18 DIV) and 17% (25 DIV) of spines contained no HA staining, with the W440A mutant spines without HA staining made up 72% (18 DIV) and 58% (25 DIV). In contrast, the fractions of the spines with high HA intensity values were not different between normal and W440A $Ca_V1.2$-HA (Fig. 6*E*). This population appears to correspond to the similarly large population of spines with high eGFP intensity (compare Fig. 6, *D* and *E*), and it is likely that these large "spines" actually represent sprouts of dendritic branches, which cannot be distinguished from large spines. Together with the altered staining pattern (Fig. 6*C*), this quantitative analysis of wild type and W440A mutant channels indicates that most, if not all, spines lack the cytoplasmic organelles containing Ca^{2+} channels en route to the plasma membrane.

Correct Subcellular Localization of β Subunits Depends on Their Interaction with an α_1 Subunit—The observation that all V5-tagged β subunits could accumulate in presynaptic terminals and colocalize with the postsynaptic $Ca_V1.2$-HA clusters suggested that the subcellular localization of the β subunits may exclusively depend on their interaction with an α_1 subunit (see above). Alternatively, specific interactions of these MAGUK proteins with pre- and postsynaptic anchoring proteins might determine their localization and in turn contribute to the specific localizations of the α_1 subunits. Coexpression of β subunits with normal and W440A mutant $Ca_V1.2$-HA now provided an experimental paradigm to test these hypotheses. We reasoned that in the absence of interactions with $Ca_V1.2$-HA(W440A), excess coexpressed β subunits will be mistargeted if their subcellular localization depends on their association with the Ca_V complex by binding the AID. This was indeed observed. Coexpression of the palmitoylated β_{2a}-V5 with $Ca_V1.2$-HA showed colocalized clusters in the dendrites (Fig. 7*A*, *left, arrowhead*) and in the axon initial segment (Fig. 7*A*, *left, arrow*). Upon coexpression with $Ca_V1.2$-HA(W440A), the clustered distribution pattern of β_{2a}-V5 was much less pronounced. Remaining weakly labeled clusters likely represent V5-tagged β subunits colocalized with clusters of endogenous channels (Fig. 7*A*, *right*). Quantitative analysis showed that the relative staining intensity was similar in neurons expressing $Ca_V1.2$-HA or $Ca_V1.2$-HA(W440A) (Fig. 7*A*, *graph*). Thus, the altered labeling pattern on coexpression of $Ca_V1.2$-HA(W440A) did not arise from reduced β expression levels but from the redistribution of the palmitoylated β_{2a} subunits in the membrane when it could not bind the AID motif of the channel.

Mutation of the N-terminal double cysteines at positions 3 and 4 to serines removed the membrane anchor of β_{2a}-SS. When coexpressed with $Ca_V1.2$-HA, both subunits colocalized in clusters at the membrane of dendrites and the initial segment of the axon (Fig. 7*B*, *arrowhead* and *arrow*, respectively). Again, coexpression with $Ca_V1.2$-HA(W440A) changed the overall distribution of β_{2a}-SS-V5 to a less intense and more uniform staining pattern. Quantitative analysis confirmed that this altered staining was due to redistribution and not reduced overall expression of β_{2a}-SS-V5 (Fig. 7*B*, *micrographs* and *graph*).

Interestingly, when coexpressed with $Ca_V1.2$-HA(W440A), a distinct accumulation of β_{2a}-SS-V5 in the most proximal part of the axon was regularly observed (Fig. 7*B*, *right, arrow*). This labeling pattern was neither observed with β_{2a}-V5 nor when β_{2a}-SS-V5 was coexpressed with the normal $Ca_V1.2$-HA. Thus, when β_{2a}-SS-V5 cannot interact with an α_1 subunit because its AID had been mutated, it is mistargeted to other neuronal structures. Together, these findings suggest that the correct subcellular localization of β subunits depends on their interaction with an α_1 subunit.

Specific Accumulation of Heterologously Expressed β_{2b} and β_{4b} in the Axon Hillock—The accumulation in the most proximal part of the axon was not unique to β_{2a}-SS-V5. Apart from their localization in pre- and postsynaptic compartments, we regularly observed a similar accumulation of β_{2b} and β_{4b} in the most proximal part of the axon when expressed without additional α_1 subunits (Fig. 7, *C* and *D*; Table 1). This staining pattern was especially pronounced in neurons expressing the β subunits at very low levels close to the limit of detection. In double staining experiments, the accumulations of β_{2b} and β_{4b} overlapped with immunolabel of voltage-gated Na^+ channels, identifying the β_{2b}- and β_{4b}-containing structure as the axon hillock (Fig. 7*D*). However, in variance with the membrane labeling pattern of the Na^+ channel, β_{2b} and β_{4b} were located in an intracellular and fibrous structure (Fig. 7*D*, *color overlay*). This is consistent with the observation that the normal palmitoylated β_{2a} did not show this staining pattern (Fig. 7*A*; see above). The fact that the β_{2a}-SS-V5 staining was primarily cytoplasmic and that it was more pronounced in combination with the $Ca_V1.2$-HA(W440A) mutant further suggests that this accumulation of β subunits in the axon hillock is not related to their association in a Ca^{2+} channel complex. Whether this phenomenon occurs with endogenous β subunits and what binding

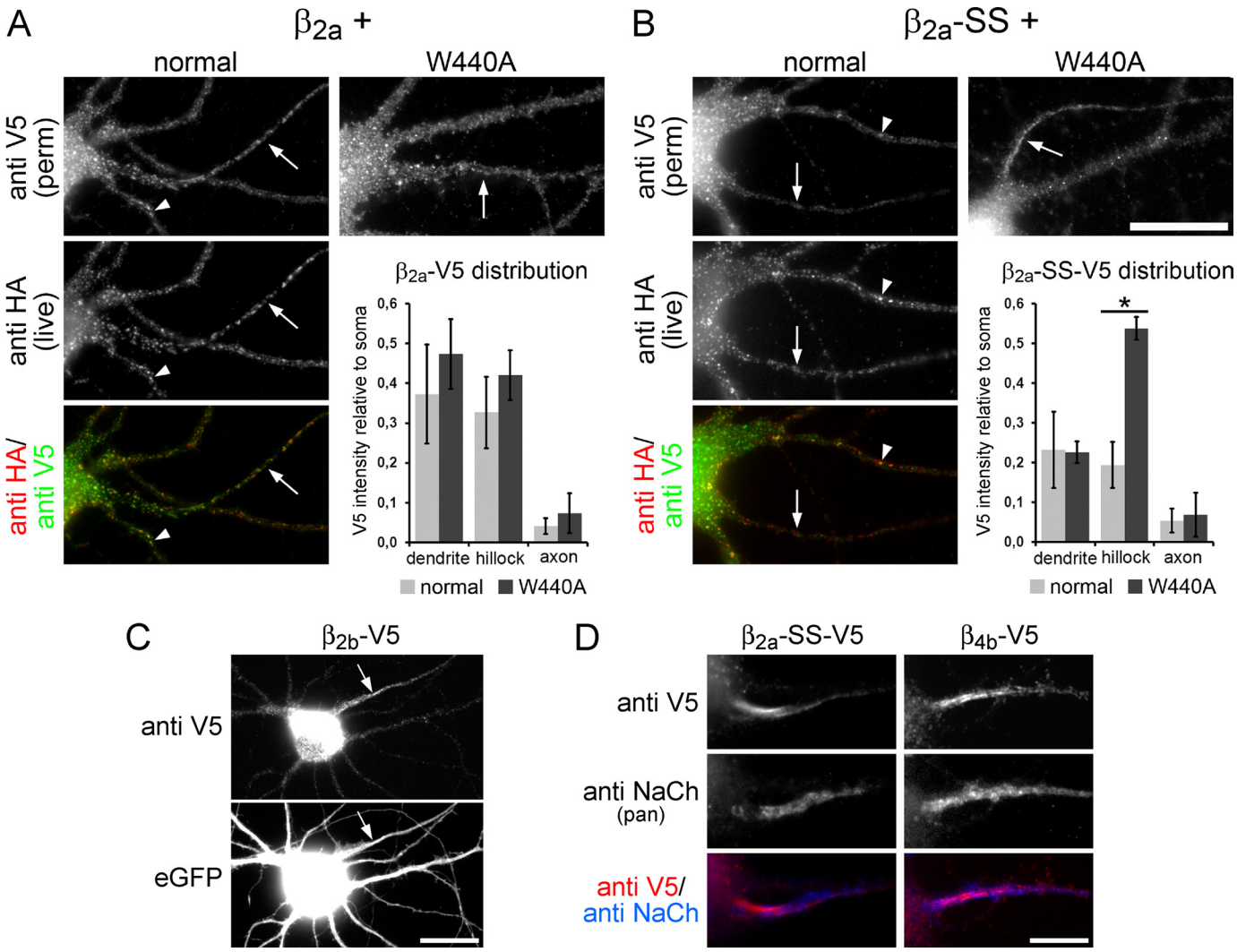

FIGURE 7. **Subcellular localization of β subunits depends on their interaction with an α_1 subunit and specific accumulation of heterologously expressed β_{2b} and β_{4b} in the axon hillock.** *A* and *B*, cultured hippocampal neurons transfected with $Ca_V1.2$-HA (*normal*) or the $Ca_V1.2$-HA(W440A) mutant (*W440A*) together with β_{2a}-V5 (*A*) or β_{2a}-SS-V5 (*B*) live cell stained with the anti-HA antibody (*anti-HA, live*) and labeled with the V5 antibody after fixation and permeabilization (*anti-V5*). *A*, β_{2a} colocalizes with membrane-incorporated $Ca_V1.2$-HA in clusters along the dendrites (*arrowhead*) and proximal axon (*arrow*). In contrast, the clustered distribution pattern of β_{2a}-V5 is less pronounced when coexpressed with $Ca_V1.2$-HA(W440A). The remaining and weakly labeled clusters likely represent V5-tagged β subunits colocalized with clusters of endogenous channels (*right*). Quantitative analysis showed that the relative staining intensity is similar in neurons expressing $Ca_V1.2$-HA or $Ca_V1.2$-HA(W440A) (*graph*: *light gray*, normal; *dark gray*, W440A). *B*, coexpression of $Ca_V1.2$-HA with the nonpalmitoylated mutant β_{2a}-SS results in similar colocalization on dendrites (*arrowhead*) and axons (*arrow*). When coexpressed with $Ca_V1.2$-HA(W440A), β_{2a}-SS-V5 labeling is enriched in the proximal part of the axon, presumably the axon hillock (*right, arrow*). This is most obvious by comparing the relative V5 intensity in the axon hillock of normal and W440A (*t* test: $t_{(23)} = -5.25$; $p < 0.001$). *C*, cultured hippocampal neuron (12 DIV) expressing β_{2b}-V5 and eGFP reveal a strong staining of β_{2b} (anti-V5) in the axon initial segment, identified based on the distinct morphology in the eGFP image (*arrow*). *D*, double labeling of cultured hippocampal neurons (19 DIV) expressing the nonpalmitoylated β_{2a}-SS-V5 mutant or β_{4b}-V5 with anti-V5 and a pan anti-Na^+ channel antibody (*anti-NaCh*) identifies the strong V5 staining in the axon hillock (see also Table 1). However, whereas the immunolabel of the membrane expressed Na^+ channel seems to envelop the axon hillock (*anti-NaCh*, *blue*), the V5 staining (*anti-V5*, *red*) appears to be restricted to an intracellular, filamentous structure. *Scale bars,* 20 μm (*B* and *C*) and 10 μm (*D*).

partners might be involved remain to be shown in future studies.

DISCUSSION

Specificity of α_1/β Pairing Is Not Determined by β Subunit Expression and Localization—Many cell types achieve exclusive α_1/β combinations by the selective expression of specific isoforms. For example, skeletal muscle expresses $Ca_V1.1$ and β_{1a}; cardiac myocytes express $Ca_V1.2$ and β_2, and retina photoreceptor cells express $Ca_V1.4$ and β_2 (2, 56). In cerebellum, $Ca_V2.1$ and β_4 are the predominant Ca_V isoforms (9, 18, 57) but not to the exclusion of others. Consistent with previous reports (17–19, 58–60), our quantitative RT-PCR analysis detected mRNA of all four β isoforms in the hippocampus. This uniform abundance does not preclude a more selective expression of β isoforms in distinct types of neurons within the hippocampal formation. Unexpectedly, however, we found that cultured hippocampal neurons, consisting of >90% glutamatergic pyramidal cells (37, 48), also expressed all four β isoforms at similar levels. Furthermore, immunofluorescence revealed similar staining patterns of the four endogenous β proteins. Together, this indicates that in cultured hippocampal neurons α_1/β subunit specificity is not the result of a selective β subunit expression pattern.

Another possible mechanism for achieving subunit specificity would be the differential targeting of β subunits into distinct compartments. Immunofluorescence analysis of the endogenous βs did not indicate such distinct localizations but showed some preference in their association with pre- and postsynaptic Ca_V α_1 subunits. Yet due to different antibodies and the inability to distinguish between splice variants, a direct comparison of labeling patterns is difficult. Expression of epitope-tagged β subunits and subsequent immunofluorescence with a single antibody presents a powerful approach to circumvent these limitations and also demonstrated a more divergent targeting behavior. On the one hand, all six examined β subunits were found in the somatodendritic and in the axonal compartment. On the other hand, β_{1a} and β_{1b} showed clearly reduced targeting into the distal axon, indicating a preferential role of β_1 in the postsynaptic compartment. The overall pattern of all β subunits was clustered and not diffuse (*cf.* Figs. 2 and 3) consistent with their localization in complexes with endogenous somatodendritic and axonal Ca_Vs, the latter possibly in vesicles or in preassembled transport packages (61).

Previous analysis of $Ca_V2.2$ splices lacking the *SYNPRINT* domain suggested the existence of separate checkpoints for axonal targeting and the incorporation of channels into the synapse (49). Also, axonal β subunits might differ in their ability to be incorporated into the presynaptic compartment. However, this was not the case. Not only were all β_2, β_3, and β_4 constructs found colocalized with the presynaptic marker synapsin, but also synapses were identified in which β_{1a} and β_{1b} were accumulated. Even though the β_1 variants were poorly targeted into distal axons, they could be incorporated into the nerve terminal like any other β subunit.

The fact that all β subunits can accumulate in presynaptic terminals suggests that they all can form complexes with presynaptic channels *in situ*. This observation is consistent with the great permissiveness of α_1-β interactions observed upon heterologous coexpression and indicates that in neurons the affinities of specific β-AID pairs (28) by themselves do not determine the specificity of α_1/β assemblies. Interestingly, low neuronal α_1/β selectivity was also suggested by immunoprecipitation experiments showing similar β subunit compositions of neuronal L-type, P/Q-type, and N-type channels (20–22).

In theory, the presynaptic accumulation of all β subunits could arise from anchoring mechanisms other than the AID of the α_1 subunits (62). The colocalization of β subunits with membrane-expressed $Ca_V1.2$-HA clusters, however, provides compelling evidence that their subcellular localization in neurons is essentially determined by this α_1-β interaction. Interestingly, upon coexpression of the W440A mutant, in which the α_1-β interaction was abolished, the localization of β subunits was altered. This result unambiguously demonstrates that specific targeting of β subunits in the postsynaptic compartment requires the interaction with the $Ca_V1.2$ α_1 subunit and that the AID is essential for this interaction. A similar conclusion was reached earlier in skeletal muscle cells, in which a Y366S mutation in the AID of $Ca_V1.1$ abolished colocalization of the β subunit but not its ability to modulate the current density (63). Together, these data indicate that an intact AID is essential for the specific localization of β subunits in nerve and muscle cells but that low affinity interactions are sufficient for current modulation by β subunits (54, 55, 64).

β Subunit Interaction at the AID Is Absolutely Required for Ca_V Membrane Expression in Neurons—Functional membrane expression of Ca_Vs in heterologous cell systems requires the presence of a β subunit (31). In contrast, only little information is available on the role of β subunits for membrane expression in the native environment of nerve cells (65). Here, we demonstrate for the first time that membrane expression of an α_1 subunit in differentiated neurons absolutely depends on its interaction with a β subunit. Membrane-incorporated $Ca_V1.2$ channels were never observed when the AID was mutated (W440A), even though the channel was expressed in cytoplasmic membrane compartments. Apparently, without a β-AID interaction, the channel is retained in the endoplasmic reticulum, as suggested previously (33). That the β requirement for membrane expression of α_1 subunits observed in heterologous cells also applies to native channels in differentiated neurons was not necessarily expected. In skeletal muscle of the immotile zebra fish mutant *relaxed*, which lacks the β subunit, this is not the case. In the absence of the β subunit $Ca_V1.1$, channels were not only incorporated into the membrane but even correctly targeted to the triadic junctions (34). Evidently, the requirement of β-AID interactions for Ca_V membrane targeting differs between nerve and muscle cells. Remarkably, membrane expression of the W440A mutant could not be rescued by coexpression of any one of the β subunits; even though coexpression with the wild type $Ca_V1.2$ resulted in a substantial increase of membrane expression. Therefore, we can conclude that putative additional binding sites, which may be specific for certain β isoforms (66), are not sufficient to induce detectable membrane expression of the channel, even if β subunits are available in excess.

Do Specific α_1/β Pairs Exist in Neurons?—Both the observation that all tested β subunits can colocalize with $Ca_V1.2$-HA in membrane clusters and the finding that β coexpression enhances membrane insertion of $Ca_V1.2$-HA underscore the general permissiveness of α_1-β interactions. Nonetheless, we also observed some remarkable β isoform-specific differences in their localization and interactions. First, β_{4b} showed a lower degree of colocalization with $Ca_V1.2$-HA than all the other β isoforms. Second, β_1 and β_2 isoforms enhanced $Ca_V1.2$-HA membrane expression more than β_3 and β_4 isoforms. Finally, β_1 was poorly transported into distal axons. Although the evidence is indirect, these subtle differences in neuronal targeting properties and in α_1-β interactions suggest that β_1 and β_2 are better partners of the somatodendritic $Ca_V1.2$ channel than β_3 and β_4; conversely, β_4 is a more likely partner for presynaptic Ca^{2+} channels than for example β_1. The latter is consistent with previous findings reporting presynaptic functions of the β_4 subunit (35, 36). Yet, neither expression patterns nor differential targeting or isoform-specific α_1-β interactions indicated the existence of explicit α_1/β pairs in hippocampal neurons. Strictly speaking, exclusive α_1/β pairs may not exist in neurons expressing multiple isoforms. However, the observed subtle differences in targeting properties and in promoting membrane expression of $Ca_V1.2$-HA, together with previously reported differences in β-AID affinities (28), may lead to the formation of

preferential α_1/β pairs. These may be in a dynamic steady state with free β subunits and change depending on the relative local concentrations of the β isoforms (67). A modest surplus of one β subunit may shift the balance toward this isoform, thus emphasizing the nonspecific, promiscuous nature of α_1-β interactions. *In vivo*, changes in relative expression levels or an activity-dependent export of free β_{4b} from the nucleus, as suggested by our recent work (70), might alter the subunit composition in one or the other neuronal compartment and thus contribute to the dynamic modulation of particular neuronal Ca^{2+} currents.

Ca_V1.2 Channels Enter Dendritic Spines via Lateral Diffusion—Finally, this study revealed the absence of cytoplasmic $Ca_V1.2$ channels from dendritic spines. Although live cell staining demonstrated that $Ca_V1.2$-HA(W440A) failed to reach the plasma membrane, staining in fixed/permeabilized neurons showed that it was distributed throughout the dendritic arbor like the wild type $Ca_V1.2$-HA. This clearly indicated that the overall $Ca_V1.2$ targeting properties are independent of an interaction with a β subunit and that Ca_Vs are inserted into the plasma membrane locally in the periphery of the neuron. However, spines of permeabilized neurons only contained $Ca_V1.2$ clusters similar to the *bona fide* membrane clusters observed in live-stained neurons but not cytoplasmic organelles containing $Ca_V1.2$. The absence of intracellular channel pools from spines suggests that $Ca_V1.2$ channels must be inserted into the membrane in the dendritic shaft and subsequently enter the spine via lateral diffusion (see model in Fig. 6). A similar pathway has recently been suggested for the α-amino-3-hydroxy-5-methyl-4-isoxazole propionate (AMPA) receptor GluR2 subunit by elegant fluorescence recovery after photobleaching studies (68). However, as opposed to the AMPA receptor, whose dynamic recycling in the postsynaptic membrane underlies synaptic plasticity, the size and density of $Ca_V1.2$ clusters in spines are stable during *N*-methyl-D-aspartic acid-induced synaptic remodeling (42).

In conclusion our data demonstrate that all four β isoforms are expressed in cultured hippocampal pyramidal neurons, are able to assemble with pre- and postsynaptic Ca_Vs, and regulate membrane expression of Ca_Vs by high affinity binding to the AID in the I–II loop of the α_1 subunit. Whereas β subunits depend on this nonspecific interaction for their own subcellular localization, additional interactions with the α_1 subunit and other binding proteins may determine β isoform-specific differences in axonal targeting and the promotion of membrane expression of neuronal Ca^{2+} channels.

Acknowledgments—We thank Dr. Veit Flockerzi for providing β_2 and β_3 antibodies, Tanja Mähr for technical assistance, and Dr. Jörg Striessnig for helpful discussions.

REFERENCES

1. Catterall, W. A. (2000) *Annu. Rev. Cell Dev. Biol.* **16,** 521–555
2. Arikkath, J., and Campbell, K. P. (2003) *Curr. Opin. Neurobiol.* **13,** 298–307
3. Stanley, E. F. (1993) *Neuron* **11,** 1007–1011
4. Dolmetsch, R. (2003) *Sci. STKE 2003*, PE4
5. Deisseroth, K., Mermelstein, P. G., Xia, H., and Tsien, R. W. (2003) *Curr. Opin. Neurobiol.* **13,** 354–365
6. Moosmang, S., Haider, N., Klugbauer, N., Adelsberger, H., Langwieser, N., Müller, J., Stiess, M., Marais, E., Schulla, V., Lacinova, L., Goebbels, S., Nave, K. A., Storm, D. R., Hofmann, F., and Kleppisch, T. (2005) *J. Neurosci.* **25,** 9883–9892
7. Witcher, D. R., De Waard, M., and Campbell, K. P. (1993) *Neuropharmacology* **32,** 1127–1139
8. Williams, M. E., Feldman, D. H., McCue, A. F., Brenner, R., Velicelebi, G., Ellis, S. B., and Harpold, M. M. (1992) *Neuron* **8,** 71–84
9. Mori, Y., Friedrich, T., Kim, M. S., Mikami, A., Nakai, J., Ruth, P., Bosse, E., Hofmann, F., Flockerzi, V., Furuichi, T., *et al.* (1991) *Nature* **350,** 398–402
10. Soong, T. W., Stea, A., Hodson, C. D., Dubel, S. J., Vincent, S. R., and Snutch, T. P. (1993) *Science* **260,** 1133–1136
11. Takahashi, M., and Catterall, W. A. (1987) *Science* **236,** 88–91
12. Hell, J. W., Westenbroek, R. E., Warner, C., Ahlijanian, M. K., Prystay, W., Gilbert, M. M., Snutch, T. P., and Catterall, W. A. (1993) *J. Cell Biol.* **123,** 949–962
13. Westenbroek, R. E., Sakurai, T., Elliott, E. M., Hell, J. W., Starr, T. V., Snutch, T. P., and Catterall, W. A. (1995) *J. Neurosci.* **15,** 6403–6418
14. Davare, M. A., Avdonin, V., Hall, D. D., Peden, E. M., Burette, A., Weinberg, R. J., Horne, M. C., Hoshi, T., and Hell, J. W. (2001) *Science* **293,** 98–101
15. Obermair, G. J., Szabo, Z., Bourinet, E., and Flucher, B. E. (2004) *Eur. J. Neurosci.* **19,** 2109–2122
16. Ruth, P., Röhrkasten, A., Biel, M., Bosse, E., Regulla, S., Meyer, H. E., Flockerzi, V., and Hofmann, F. (1989) *Science* **245,** 1115–1118
17. Perez-Reyes, E., Castellano, A., Kim, H. S., Bertrand, P., Baggstrom, E., Lacerda, A. E., Wei, X. Y., and Birnbaumer, L. (1992) *J. Biol. Chem.* **267,** 1792–1797
18. Castellano, A., Wei, X., Birnbaumer, L., and Perez-Reyes, E. (1993) *J. Biol. Chem.* **268,** 12359–12366
19. Castellano, A., Wei, X., Birnbaumer, L., and Perez-Reyes, E. (1993) *J. Biol. Chem.* **268,** 3450–3455
20. Liu, H., De Waard, M., Scott, V. E., Gurnett, C. A., Lennon, V. A., and Campbell, K. P. (1996) *J. Biol. Chem.* **271,** 13804–13810
21. Pichler, M., Cassidy, T. N., Reimer, D., Haase, H., Kraus, R., Ostler, D., and Striessnig, J. (1997) *J. Biol. Chem.* **272,** 13877–13882
22. Scott, V. E., De Waard, M., Liu, H., Gurnett, C. A., Venzke, D. P., Lennon, V. A., and Campbell, K. P. (1996) *J. Biol. Chem.* **271,** 3207–3212
23. Ludwig, A., Flockerzi, V., and Hofmann, F. (1997) *J. Neurosci.* **17,** 1339–1349
24. Hanlon, M. R., Berrow, N. S., Dolphin, A. C., and Wallace, B. A. (1999) *FEBS Lett.* **445,** 366–370
25. Opatowsky, Y., Chomsky-Hecht, O., Kang, M. G., Campbell, K. P., and Hirsch, J. A. (2003) *J. Biol. Chem.* **278,** 52323–52332
26. Van Petegem, F., Clark, K. A., Chatelain, F. C., and Minor, D. L., Jr. (2004) *Nature* **429,** 671–675
27. Chen, Y. H., Li, M. H., Zhang, Y., He, L. L., Yamada, Y., Fitzmaurice, A., Shen, Y., Zhang, H., Tong, L., and Yang, J. (2004) *Nature* **429,** 675–680
28. De Waard, M., Witcher, D. R., Pragnell, M., Liu, H., and Campbell, K. P. (1995) *J. Biol. Chem.* **270,** 12056–12064
29. Pragnell, M., De Waard, M., Mori, Y., Tanabe, T., Snutch, T. P., and Campbell, K. P. (1994) *Nature* **368,** 67–70
30. Colecraft, H. M., Alseikhan, B., Takahashi, S. X., Chaudhuri, D., Mittman, S., Yegnasubramanian, V., Alvania, R. S., Johns, D. C., Marbán, E., and Yue, D. T. (2002) *J. Physiol.* **541,** 435–452
31. Dolphin, A. C. (2003) *J. Bioenerg. Biomembr.* **35,** 599–620
32. Lacerda, A. E., Kim, H. S., Ruth, P., Perez-Reyes, E., Flockerzi, V., Hofmann, F., Birnbaumer, L., and Brown, A. M. (1991) *Nature* **352,** 527–530
33. Bichet, D., Cornet, V., Geib, S., Carlier, E., Volsen, S., Hoshi, T., Mori, Y., and De Waard, M. (2000) *Neuron* **25,** 177–190
34. Schredelseker, J., Di Biase, V., Obermair, G. J., Felder, E. T., Flucher, B. E., Franzini-Armstrong, C., and Grabner, M. (2005) *Proc. Natl. Acad. Sci. U.S.A.* **102,** 17219–17224
35. Wittemann, S., Mark, M. D., Rettig, J., and Herlitze, S. (2000) *J. Biol. Chem.* **275,** 37807–37814
36. Xie, M., Li, X., Han, J., Vogt, D. L., Wittemann, S., Mark, M. D., and Herlitze, S. (2007) *J. Cell Biol.* **178,** 489–502

37. Obermair, G. J., Kaufmann, W. A., Knaus, H. G., and Flucher, B. E. (2003) *Eur. J. Neurosci.* **17,** 721–731
38. Fischer, M., Kaech, S., Knutti, D., and Matus, A. (1998) *Neuron* **20,** 847–854
39. Pragnell, M., Sakamoto, J., Jay, S. D., and Campbell, K. P. (1991) *FEBS Lett.* **291,** 253–258
40. Koschak, A., Obermair, G. J., Pivotto, F., Sinnegger-Brauns, M. J., Striessnig, J., and Pietrobon, D. (2007) *J. Neurosci.* **27,** 3855–3863
41. Sinnegger-Brauns, M. J., Huber, I. G., Koschak, A., Wild, C., Obermair, G. J., Einzinger, U., Hoda, J. C., Sartori, S. B., and Striessnig, J. (2009) *Mol. Pharmacol.* **75,** 407–414
42. Di Biase, V., Obermair, G. J., Szabo, Z., Altier, C., Sanguesa, J., Bourinet, E., and Flucher, B. E. (2008) *J. Neurosci.* **28,** 13845–13855
43. Watschinger, K., Horak, S. B., Schulze, K., Obermair, G. J., Wild, C., Koschak, A., Sinnegger-Brauns, M. J., Tampé, R., and Striessnig, J. (2008) *Channels* **2,** 461–473
44. Flucher, B. E., Andrews, S. B., Fleischer, S., Marks, A. R., Caswell, A., and Powell, J. A. (1993) *J. Cell Biol.* **123,** 1161–1174
45. Di Biase, V., Flucher, B. E., and Obermair, G. J. (2009) *J. Neurosci. Methods* **176,** 78–84
46. Li, Q., Lau, A., Morris, T. J., Guo, L., Fordyce, C. B., and Stanley, E. F. (2004) *J. Neurosci.* **24,** 4070–4081
47. Bolte, S., and Cordelières, F. P. (2006) *J. Microsc.* **224,** 213–232
48. Benson, D. L., Watkins, F. H., Steward, O., and Banker, G. (1994) *J. Neurocytol.* **23,** 279–295
49. Szabo, Z., Obermair, G. J., Cooper, C. B., Zamponi, G. W., and Flucher, B. E. (2006) *Eur. J. Neurosci.* **24,** 709–718
50. Fletcher, T. L., Cameron, P., De Camilli, P., and Banker, G. (1991) *J. Neurosci.* **11,** 1617–1626
51. Chien, A. J., and Hosey, M. M. (1998) *J. Bioenerg. Biomembr.* **30,** 377–386
52. Qin, N., Platano, D., Olcese, R., Costantin, J. L., Stefani, E., and Birnbaumer, L. (1998) *Proc. Natl. Acad. Sci. U.S.A.* **95,** 4690–4695
53. De Waard, M., Scott, V. E., Pragnell, M., and Campbell, K. P. (1996) *FEBS Lett.* **380,** 272–276
54. Leroy, J., Richards, M. W., Richards, M. S., Butcher, A. J., Nieto-Rostro, M., Pratt, W. S., Davies, A., and Dolphin, A. C. (2005) *J. Neurosci.* **25,** 6984–6996
55. Butcher, A. J., Leroy, J., Richards, M. W., Pratt, W. S., and Dolphin, A. C. (2006) *J. Physiol.* **574,** 387–398
56. Ball, S. L., Powers, P. A., Shin, H. S., Morgans, C. W., Peachey, N. S., and Gregg, R. G. (2002) *Invest. Ophthalmol. Vis. Sci.* **43,** 1595–1603
57. Starr, T. V., Prystay, W., and Snutch, T. P. (1991) *Proc. Natl. Acad. Sci. U.S.A.* **88,** 5621–5625
58. Witcher, D. R., De Waard, M., Liu, H., Pragnell, M., and Campbell, K. P. (1995) *J. Biol. Chem.* **270,** 18088–18093
59. Burgess, D. L., Biddlecome, G. H., McDonough, S. I., Diaz, M. E., Zilinski, C. A., Bean, B. P., Campbell, K. P., and Noebels, J. L. (1999) *Mol. Cell. Neurosci.* **13,** 293–311
60. Tanaka, O., Sakagami, H., and Kondo, H. (1995) *Brain Res. Mol. Brain Res.* **30,** 1–16
61. Ahmari, S. E., Buchanan, J., and Smith, S. J. (2000) *Nat. Neurosci.* **3,** 445–451
62. Vendel, A. C., Terry, M. D., Striegel, A. R., Iverson, N. M., Leuranguer, V., Rithner, C. D., Lyons, B. A., Pickard, G. E., Tobet, S. A., and Horne, W. A. (2006) *J. Neurosci.* **26,** 2635–2644
63. Neuhuber, B., Gerster, U., Döring, F., Glossmann, H., Tanabe, T., and Flucher, B. E. (1998) *Proc. Natl. Acad. Sci. U.S.A.* **95,** 5015–5020
64. Gerster, U., Neuhuber, B., Groschner, K., Striessnig, J., and Flucher, B. E. (1999) *J. Physiol.* **517,** 353–368
65. Berrow, N. S., Campbell, V., Fitzgerald, E. M., Brickley, K., and Dolphin, A. C. (1995) *J. Physiol.* **482,** 481–491
66. Walker, D., and De Waard, M. (1998) *Trends Neurosci.* **21,** 148–154
67. Obermair, G. J., Tuluc, P., and Flucher, B. E. (2008) *Curr. Opin. Pharmacol.* **8,** 311–318
68. Jaskolski, F., Mayo-Martin, B., Jane, D., and Henley, J. M. (2009) *J. Biol. Chem.* **284,** 12491–12503
69. Goslin, K., Asmussen, H., and Banker, G. (1998) in Culturing Nerve Cells (Banker, G., and Goslin, K., eds) pp. 339–370, MIT Press, Cambridge, MA
70. Subramanyam, P., Obermair, G. J., Baumgartner, S., Gebhart, M., Striessnig, J., Kaufmann, W. A., Geley, S., and Flucher, B. E. (2009) *Channels* **3,** 343–355